To the Graduate Council:

I am submitting herewith a thesis written by Navin Tyle entitled "Control of a Commercial Scale MHD/Steam Power Plant." I recommend that it be accepted in partial fulfillment of the requirements for the degree of Master of Science, with a major in Electrical Engineering.

Roy D. Joseph, Major Professor

We have read this thesis
and recommend its acceptance:

Accepted for the Council:

Vice Chancellor
Graduate Studies and Research

CONTROL OF A COMMERCIAL SCALE MHD/STEAM POWER PLANT

A Thesis
Presented for the
Master of Science
Degree
The University of Tennessee, Knoxville

Navin Tyle

August 1980

ACKNOWLEDGEMENTS

The valuable guidance, suggestions and encouragement given by Dr. Roy D. Joseph, Major Professor are acknowledged with deep gratitude. The tutorial guidance on MHD by Dr. James N. Chapman and Dr. Ying-Chu Lin Wu is highly appreciated. The author is also very grateful to Dr. Eugene C. Huebschman for his assistance and encouragement during the one year of graduate work.

Sincere thanks are extended to James R. Hollis for his supervision and guidance during the period of author's association with the Systems studies group. Help given by Edward H. Kiessling III is very much appreciated.

The work reported herein was supported by the U.S. Department of Energy, contract number DE-AC02-79ET10815.

ABSTRACT

A model for a commercial scale 1000 MW_e MHD/Steam power plant was developed and used to study control problems.

To determine the behavior of the system state variables in the presence of load demand perturbations, a linear incremental model was contructed for the plant. The model made use of a fuel dependent MHD channel and the known characteristics of the downstream steam plant.

Using the Megawatt-Frequency concept, various control techniques for dealing with a step change in electric load demand were studied. Both continous and digital control functions were applied to limit the frequency deviation on the utility grid.

It was found that the fuel and air inputs to the combustor are sufficient to control the plant. The large lags in the steam section are overcome by the relatively fast response of the MHD section and result in a satisfactory transient response with no auxiliary boiler present.

By using only proportional-integral-derivative (PID) control, the simulated plant settled to a new steady state point within 35-50 seconds. Optimal state variable feedback gave a low settling time (40-60 seconds) with a reduced control effort. A peak control criteria was used to select an acceptable continous control technique.

For digital control, a finite-time settling time control algorithm was applied to the discrete plant model. For sampling periods of one to five seconds, the plant settles to a new steady state in 10-50 seconds with acceptable level of control effort. This technique is recommended for real time process control of the combined MHD/Steam power plant.

TABLE OF CONTENTS

LIST OF TABLES

LIST OF FIGURES

NOMENCLATURE

α	Weight on the frequency error
A, A_d	System matrix
$\underline{B}$, $\underline{h}$	Input vector
C_3	Coefficient of the derivative term
Δ	Change in a quantity
e_f	Frequency error
e_u	Total control effort
f	System frequency
J	Cost function
P_d	Power demand
P_i	Inverter output electric power
PID	Proportional-Integral-Derivative control
P_s	Steam section output electric power
p_u	Peak control effort
T	Sampling interval
u	Control input
W_{fuel}	Fuel input flow rate
$\underline{x}$, $\underline{x}'$	State variables
X_3	Power mismatch

CHAPTER I

INTRODUCTION

1. MHD GENERATOR CONFIGURATION

The United States has abundant coal reserves to supply the majority of its total energy needs. The binary MHD/Steam energy conversion is an efficient technique for utilizing coal to supply these needs.

The magnetohydrodynamic generator transforms the internal energy of a gas into electric power by expanding the gas and passing it through a magnetic field. The four basic types of linear open-cycle MHD generators are shown in Figure 1. These configurations have been shown to be of use in central power generation (1). They include (2):

1. Continous Electrode Faraday Generator
2. Segmented Electrode Faraday Generator
3. Hall Generator
4. Diagonal Conducting Wall Generator (DCW)

The continous electrode and Hall generators have been found unsuitable for power generation applications (1). The segmented elctrode generator requires a separate inverter circuit for each pair of elctrodes resulting in additional cost. For these reasons all known system studies (3,4,5,6) have proposed to utilize the Diagonal conducting wall configuration. This study will utilize the DCW generator operating with a single load.

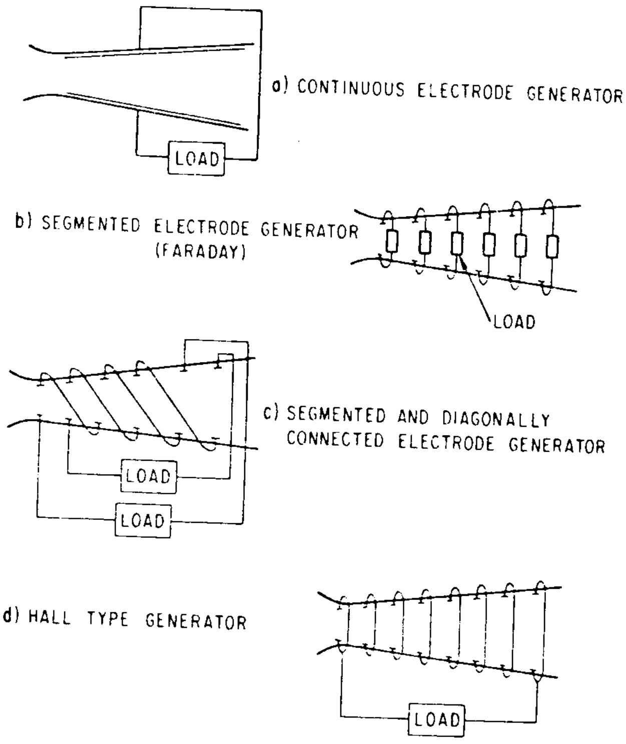

Figure 1. Basic types of Linear MHD generators

For the interested reader, a detailed review of the evidence leading to this choice has been prepared (6).

2. MHD/STEAM PLANT CONFIGURATION

Figure 2 is a schematic of a commercial scale open-cycle MHD/Steam power plant (7). The major components are:

1. Combustor
2. MHD Channel
3. Magnet (Superconducting)
4. Inverters and Power conditioners
5. Diffuser
6. Heat recovery system including air preheaters
7. Gasifier and High Temperature air heaters
8. Steam bottoming cycle
9. Seed collection and regeneration system

Air is compressed in the main steam driven compressors and then preheated in the heat recovery system and in the high temperature air heaters (HTAH). Pulverized coal is mixed with a small amount of potassium seed (K_2CO_3) and is burnt with the hot air, in a fuel rich environment, in the combustor. The resulting high temperature plasma (at approximately 3000°K) is then accelerated to near sonic velocity in the nozzle and allowed to flow into the MHD channel. The DC power generated is converted to AC power for feeding to the utility line.

The hot gases are decelerated in the diffuser and then enter the heat recovery system where they lose heat to the

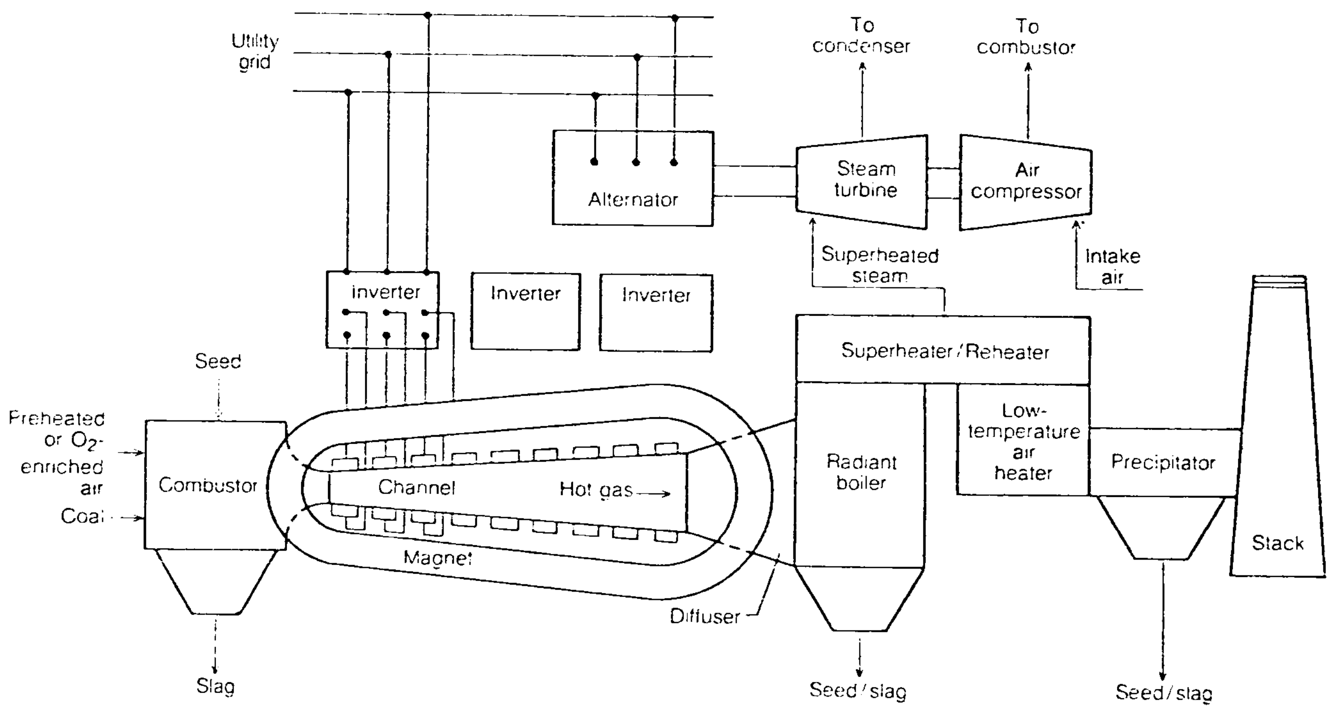

Figure 2. A schematic of a MHD/Steam power plant

boiler feed water and to the air. The seed material which is converted to the sulphate form is removed before the exhaust goes out of the stack. This is then circulated to the seed regeneration system to convert back to carbonate form for use again.

The air is preheated in the heat recovery system and then in the high temperature air heaters to about 1900°K. The HTAH are externally fired, regenerative air heaters run on clean, low BTU fuel gas produced by the coal gasifiers.

The steam generated in the heat recovery system, the seed regeneration system and the gasifiers is used to drive the air compressors and a turbogenerator producing AC electric power directly. This section of the plant is referred to as the steam bottoming plant. The spent steam from the turbine is condensed and heat discharged in wet cooling towers.

Such a combined plant promises an overall efficiency of 43-50% compared to an efficiency of 33-35% for a coal fired thermal power plant with flue gas desulpherization (8).

3. REVIEW OF CONTROL SYSTEM DESIGN

Most of the studies in the past have emphasized the development of system simulation models in terms of mass and heat flow rates. Economic and physical description models have been constructed by Chapman (9), Hals (10), Hollis et al. (11), Oliver and Byer (12), Zygielbaum (13) and others. Robles (14) and various other research workers have developed quasi-one dimensional models for the combined plant without any control system considerations. Aspens (15) has made a fairly sophisticated model and has applied classical control techniques. Agarwal (16) recently applied classical and modern control theory to a representative MHD/Steam system. No work, however, has been reported on the direct digital control of the combined plant, especially of the commercial scale.

4. SCOPE OF PRESENT WORK

The purpose of this work is the development of an incremental power model for a commercial scale MHD/Steam power plant that is sufficiently accurate for the study of control applications. A diagonal conducting wall MHD generator is modeled and fuel dependent load lines obtained. This together with the steam plant characteristics leads to an incremental power model for the overall plant. The combined plant is assumed to feed base load requirements implying the changes in the load demand are step type and are of small value.

The two following important characteristics about the plant are known (17) :

1. A mismatch in real power, P affects primarily the system frequency but leaves the voltage magnitudes basically unaffected.

2. A mismatch in reactive power, Q affects only the bus voltage magnitudes but leaves the system frequency unchanged.

It is emphasized that these two conditions apply for small deviations in the power demand. In view of these facts, the control problem can be divided into two decoupled and independent problems :

1. The Megawatt-Frequency control problem or the PF problem. Here the frequency deviation is sensed on the bus and the real power generation is accordingly changed by the control system action.

2. The Megavar-Voltage control problem or the QV problem. The bus voltage magnitude deviation is sensed, this being the most indicative of reactive power imbalance. If an error exists, reactive power produced is controlled by the field excitation of the rotating machinery and by the additional reactive power sources in the system.

The MHD/Steam power plant presents unique PF control problem since only the steam section has any rotating machines. The QV problem is usually solved with conventional control techniques of changing the field winding current of the steam generator. We will not consider this aspect of power control in this study. We will study various control applications for the solution of the PF problem. The classical and modern control systems are found to give acceptable system performance in this study.

CHAPTER II

STEADY STATE SYSTEM MODELING

Steady state performance evaluation includes the design of an appropriate MHD generator and the selection of other plant components as were shown in Figure 2.

1. MHD GENERATOR DESIGN

A Diagonal Conducting Wall generator (DCW) to be used in the 1000 MW_e combined plant was designed using the DESIGN3 numerical simulation program (18). This computer program simulates a quasi-one dimensonal MHD generator model under steady state. The DCW generator output is optimized by varying the load current. A load current of 25000 amperes was found to maximize the power output under constraints on various flow parameters. The steady state plasma flow rate in the MHD channel was 488 kg/sec (3.8×10^6 lb/hr) corresponding to a coal flow input rate of 54.4 kg/sec (1.96×10^5 lb/hr) into the MHD combustor. The generator was designed on the basis of this mass flow rate for the plasma.

The velocity of the plasma in the channel was always kept below the sonic speed. The flow mach number variation, magnetic field configuration and the voltage variation along the length of the channel are shown in Figure 3.

During the transient period, when the load demand is

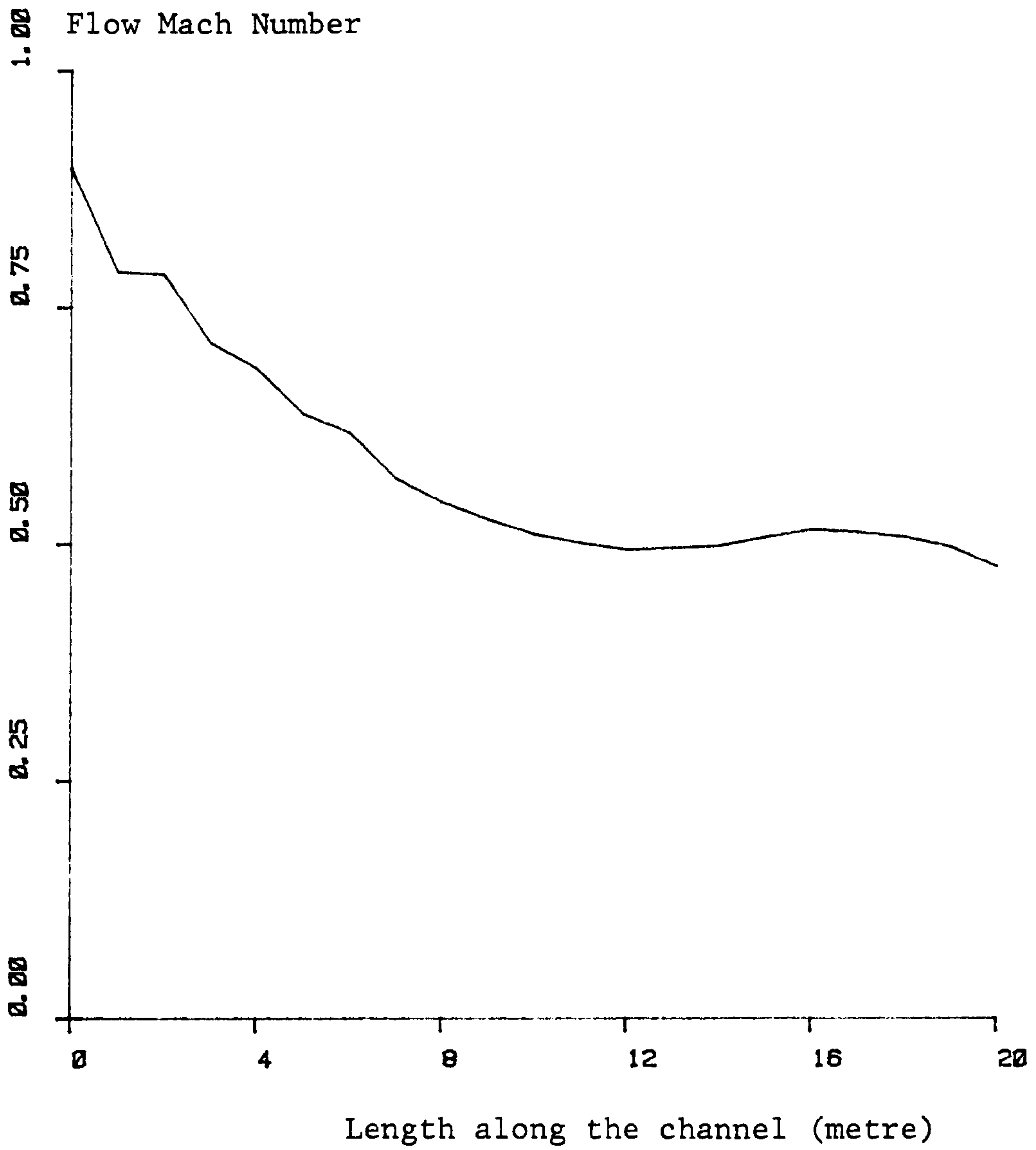

Figure 3. MHD channel characteristics

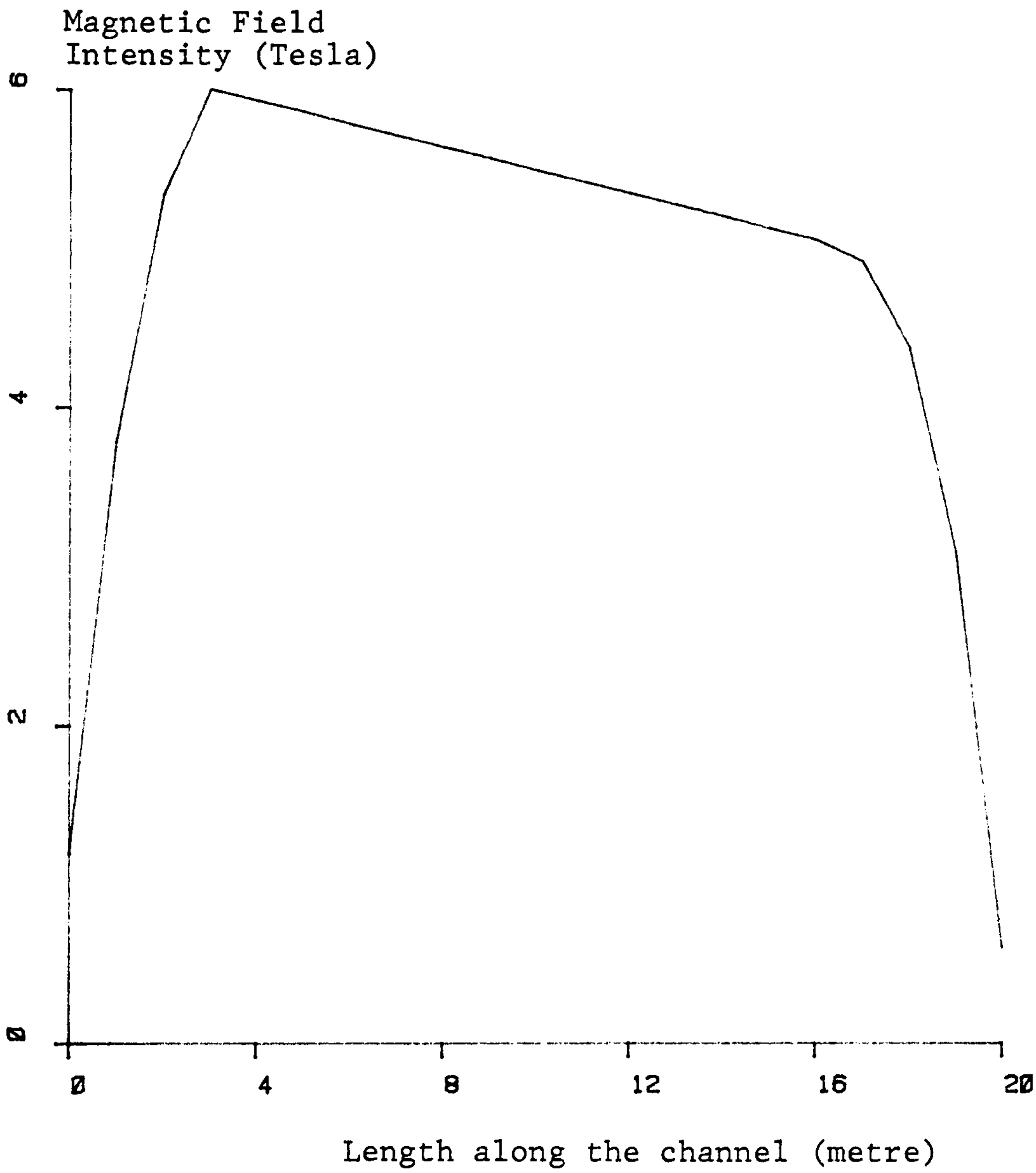

Figure 3. (continued)

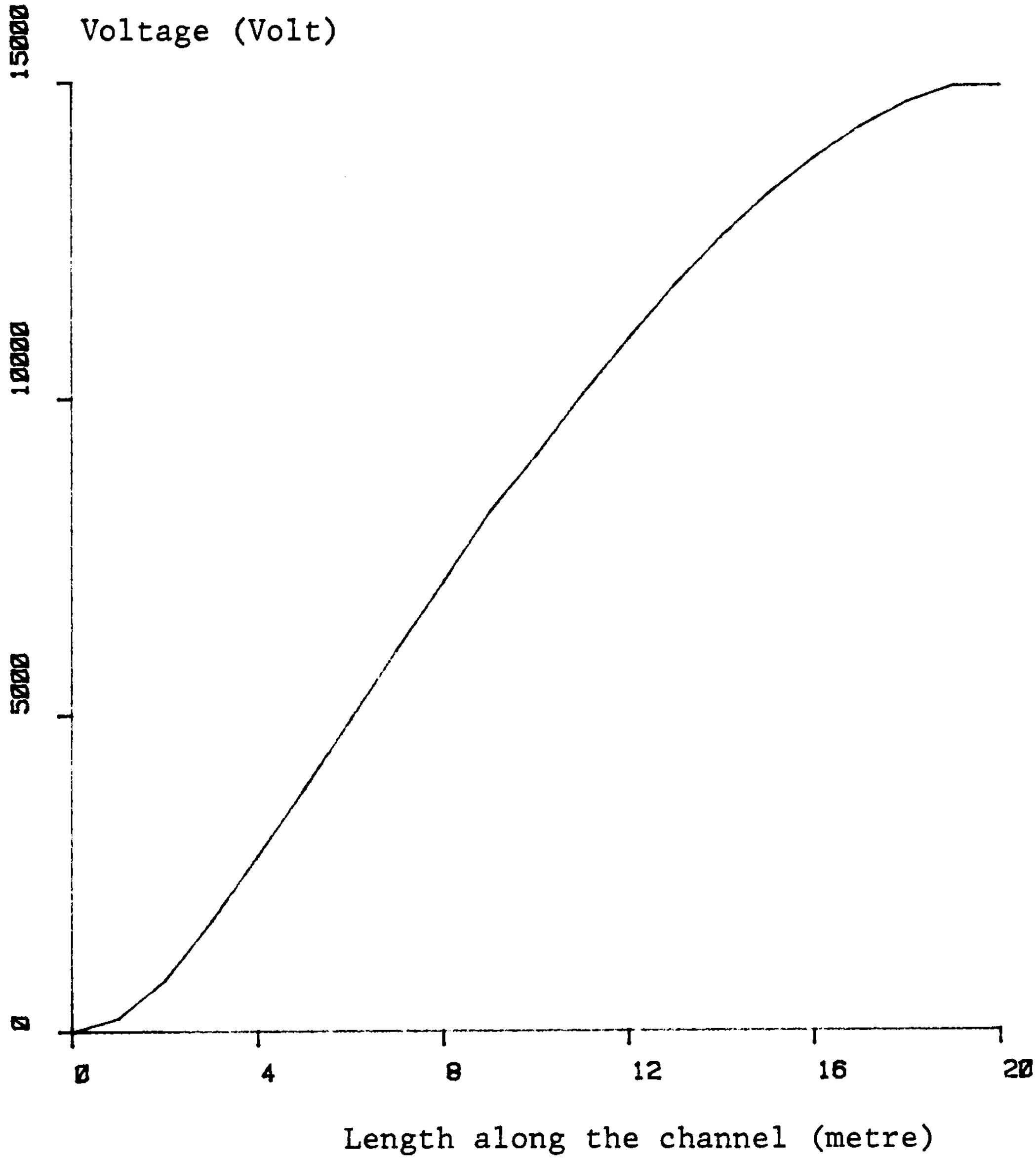

Figure 3. (continued)

varying, the fuel input to the plant is controlled. In order to obtain an incremental power model of the MHD channel, its fuel dependent behavior was studied. Fuel input rate was varied ± 5% about the steady state value of 54.4 kg/sec, and the load lines were obtained. The voltage versus load current variation is shown in Figure 4. The power output of the channel also varies as the fuel input rate is varied. This variation is shown in Figure 5. The optimal steady state point is marked at a load current of 25000 amperes. As the fuel input is changed the power output will remain optimal if the load is kept the same. This constant load corresponds to the resistance line superimposed on the curves in Figure 4 and 5. Based on the power output curves, a constant K signifying the change in output power per unit change in input fuel flow rate, is calculated as shown in Figure 5. This constant will be used to model the incremental power behavior of the MHD channel. It is possible to do so, since the load lines are fairly linear within the range of load variation considered in this study.

2. MHD/STEAM PLANT SIMULATION

A generalized steady state model representing the combined plant was developed and is described in references (11,19). The Appendix describes the actual plant model used for the study of the steady state performance of the combined MHD/Steam power plant.

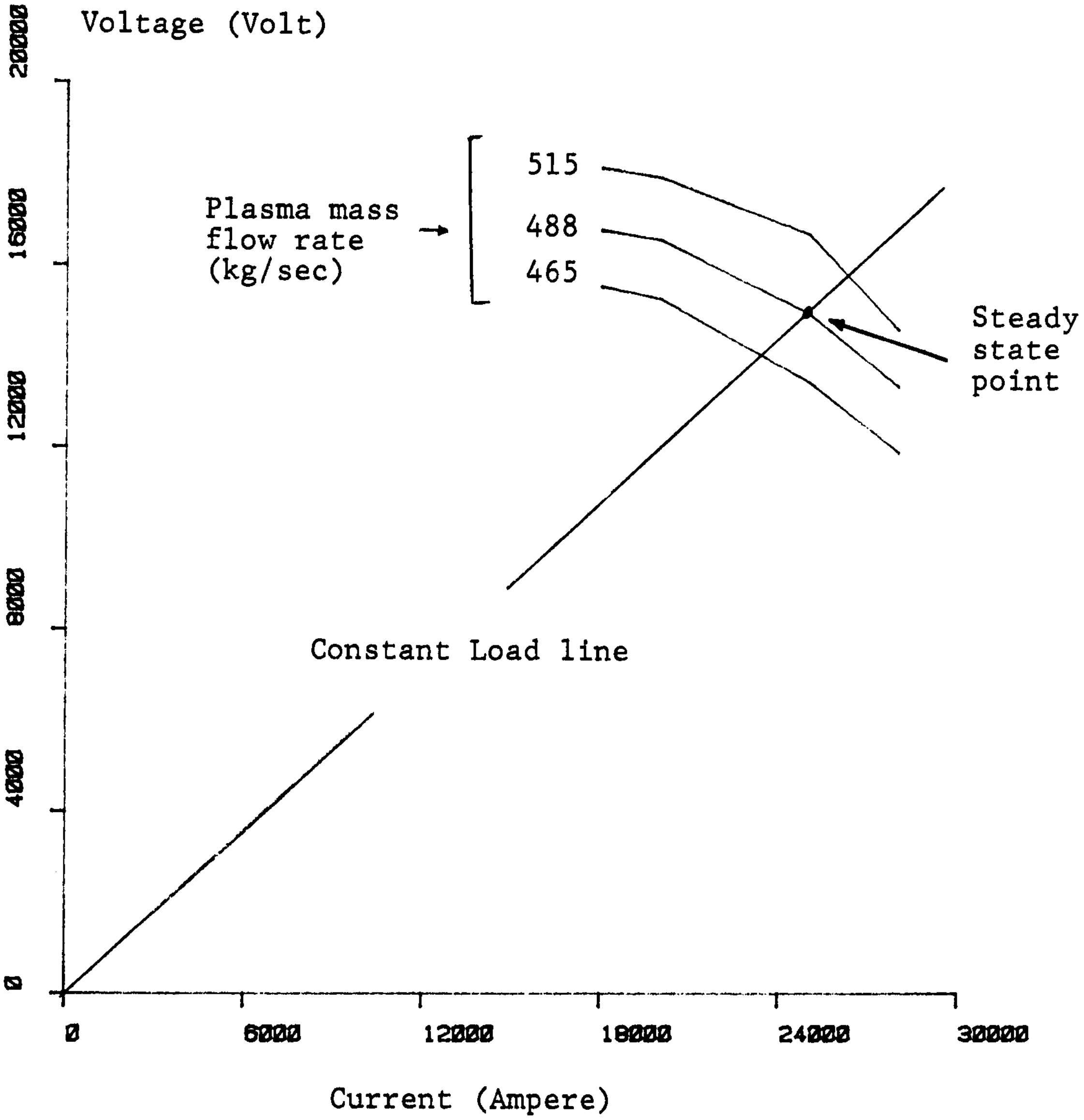

Figure 4. Load line characteristics

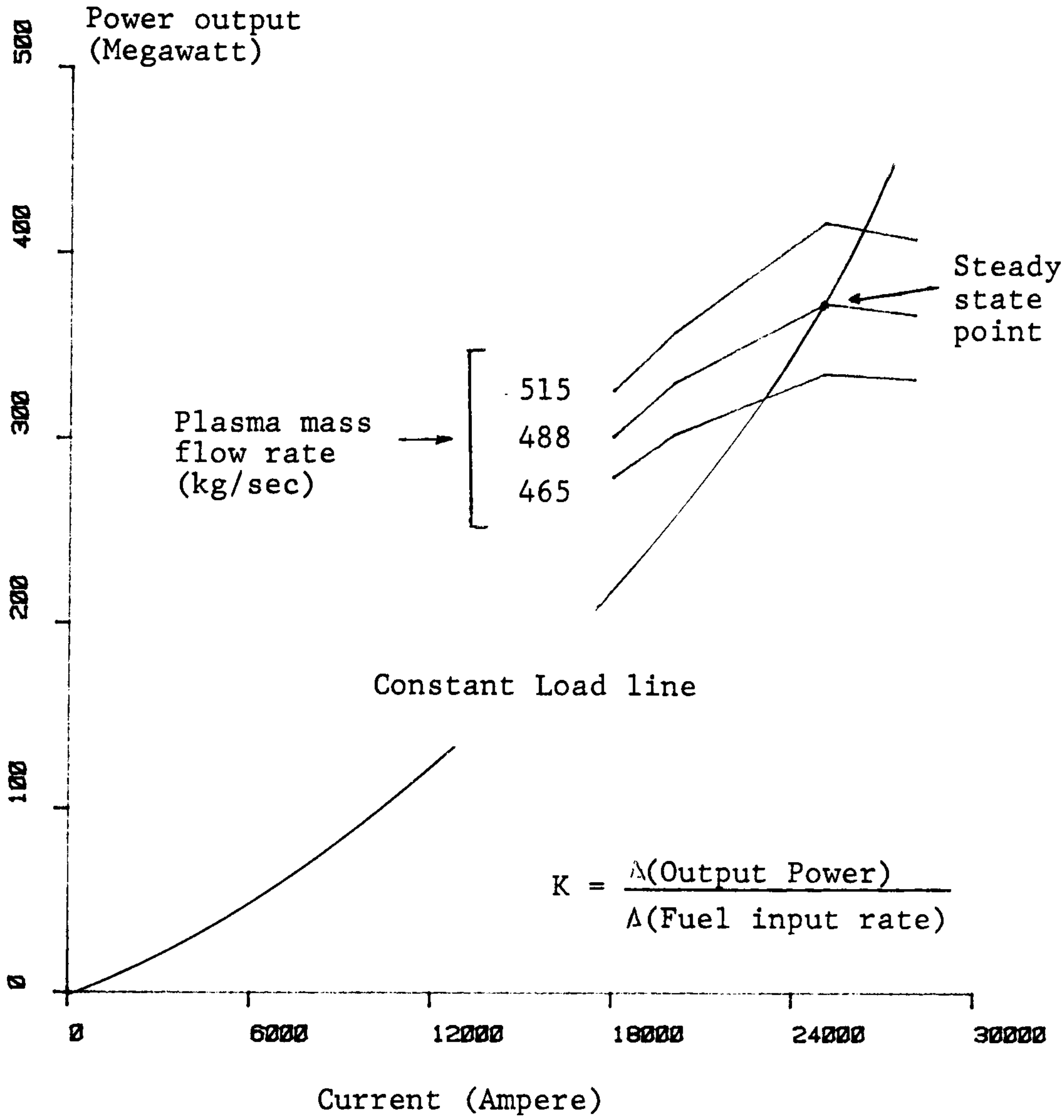

Figure 5. Output power characteristics

The parameters used for the steady state model of the combined plant are listed in Table 1. Illinois # 6 coal is used with the already designed DCW generator. The input specifications to the performance model include the plant output power, coal and oxidant composition and ratio, MHD generator parameters and the air preheat temperature. The major steps in the calculation procedure are listed in Table 2. The procedure calculates the performance of each of the plant components. The plant design is revised until the desired specifications are met completely. It also calculates the capital and operating costs for the plant. A power summary for the plant is given in Table 3. These power flows are for the steady state operating conditions. These values are utilized in the development of the incremental power model.

It is noted from Table 3 that the MHD and the steam section contribute to the total power output in the approximate ratio of 40/60 respectively.

TABLE 1

MAJOR DESIGN PARAMETERS OF THE COMBINED PLANT

Plant Parameter	Units	Description
Plant Size	MW_e	1000
Fuel		Illinois # 6 coal
MHD Combustor		
Fuel		Pulverized Coal
Fuel Moisture Content	%	2.0
Oxidizer		Air (21% oxygen)
Oxidant/Fuel ratio		0.84
Air Preheater		
Type		Indirect HTAH
Temperature (Air)	°K	1922
Fuel		Low BTU gas
Gasifier		
Type		Entrained Bed
Fuel		Illinois # 6 coal
MHD Generator		
Type		Diagonal Conducting Wall
Magnetic Field	Tesla	6.0 (maximum)
Seed Proportion	%	1.0 (maximum)
Flow velocity		Subsonic
Steam Bottoming Cycle		
Pressure	psi	2400
Temperature	°K	811
Reheat Temperature	°K	811
Seed Regeneration System		
Type		Tomlinson Tempella Process

TABLE 2

STEADY STATE PERFORMANCE COMPUTATION PROCEDURE

Step	Description
I.	Design of an optimal DCW generator.
II.	Thermodynamic properties computation using the procedure in reference (20).
III.	Input specifications to the steady state performance model: 1. Generator parameters 2. Component indicators 3. Thermodynamic coefficients 4. Plant configuration
IV.	Execution of component subroutines in the same order as specified in step III. Compute component performance parameters.
V.	Check if the output specifications have been met by the design. If no, make a change in fuel input mass flow rate and return to step I.
VI.	Calculate capital and operating costs for the plant design selected.
VII.	Print results.

TABLE 3

OVERALL PLANT ENERGY BALANCE

Description of Flow	Input (MW)	Output (MW)
Heat Input		
Coal to MHD combustor	1528.38	
Coal to Gasifier	847.68	
Coal to seed regeneration	188.11	
Total power input	2564.17	
Electrical Output		
MHD output power		413.71
Steam output power		590.52
System losses		
Auxiliary power		56.50
Heat recovery system loss		42.56
Heat rejected to stack		116.61
Heat rejected in condenser		1199.66
Gasifier and HTAH loss		38.37
Seed regeneration system loss		47.88
Slag heat loss		15.77
Inverter loss		12.79
Other losses		29.80
Total Output (Electric + Losses)		2564.17

CHAPTER III

INCREMENTAL POWER MODELING

The combined plant is assumed to be operating at a steady state point, and that it is connected to a commercial grid whose capacity is several times larger than that of the plant under study.

As discussed in Chapter I, changes in the real power demand affect the system frequency f. The purpose of PF control is to steer the system to a new steady state such that the frequency deviation Δf settles down to zero. When a change in real power demand is received the PF control will vary the fuel input rate to the plant. This is because one of the most reasonable ways by which the power demand change ΔP_d can be met is by changing the power input to the plant i.e. by changing the coal, preheated air and seed input flow rates.

1. MHD GENERATOR-INVERTER INCREMENTAL MODEL

The output of an MHD generator can be controlled by the mass flow of the input fuel, the firing angle of the inverter or by the use of a load-tap changing transformer (LTC).

Control of the firing angle is rapid (1 to 10 millisecond), but the LTC transformer is a slow changing controller (5 to 6 seconds). Hence the former is used initially for rapid control action and is followed by the LTC transformer for restoring the system once the new steady state is attained (21).

Figure 6 shows a plot of ideal load line characteristics of a MHD generator on a normalized voltage, current and power scale. Superimposed on the MHD generator load lines are the characteristics of the current fed inverter system. The line A'B' is the natural voltage line of the inverter and the 1.0 PU power line is the natural load line of the channel. If the MHD dynamics try to move it downwards, due to decrease in the power input, the inverter will automatically shift to the 'Current control' mode of operation on line A'''B''' and still maintain the maximum possible power output. Similarly if the power output increases and MHD load line shifts to 1.28 PU line, the inverter characteristics shift to line A''B''. This automatic control of the inverter system is accomplished by a feedback control network shown in Figure 7 (21,22). In this controller, the reference voltage and current is compared the corresponding actual values and the firing angle of the inverter controlled. This results in a fast change in the MHD power output. However, the LTC transformer or a suitable solid state alternative (23) is used once the transient period is over and a new steady state has been reached.

The load line characteristics of the DCW generator used in the design of the combined plant have already been seen to be linear in the vicinity of the operating point. If we assume that the inverter system is controlled in the manner described above, the effect of fuel input change on the load impedance

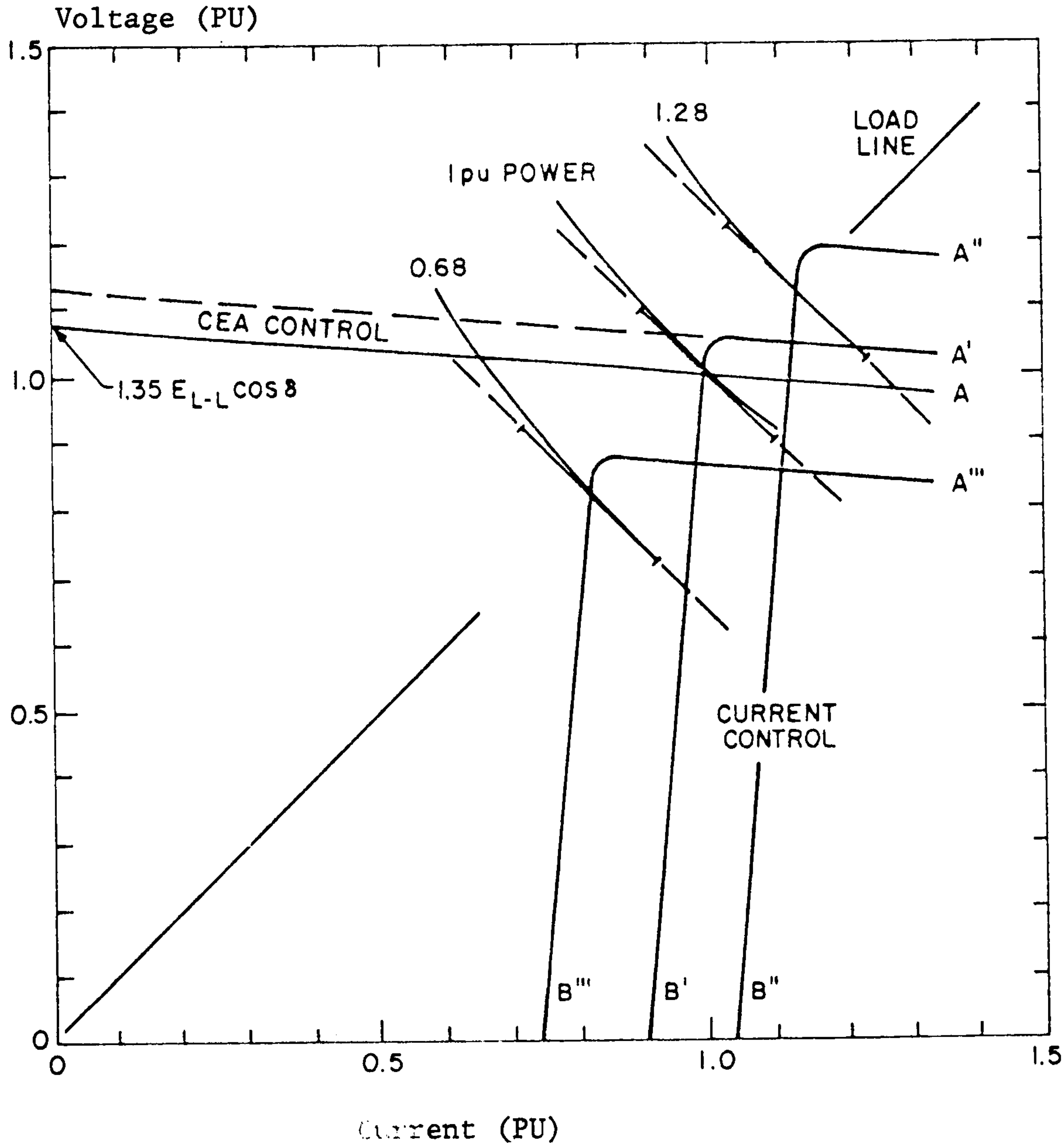

Figure 6. Ideal MHD Generator-Inverter characteristics

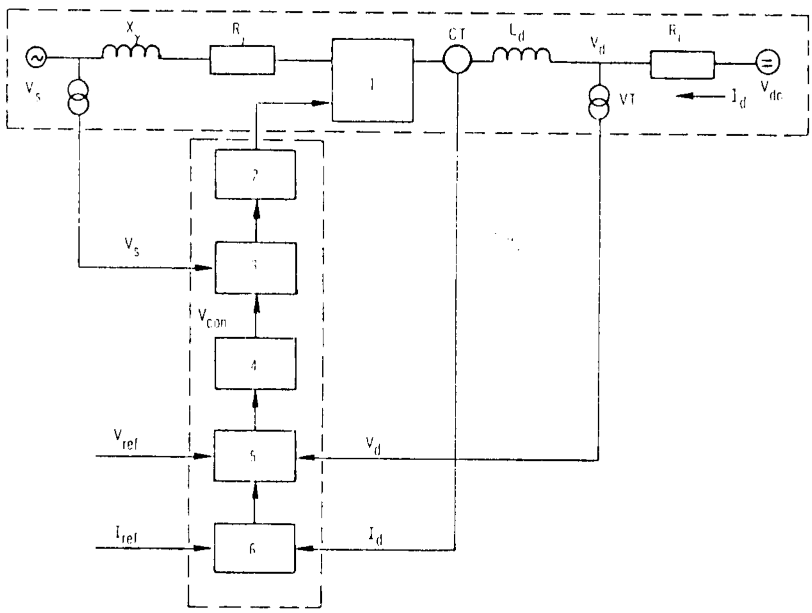

Figure 7. Automatic Inverter control system

1 = Inverter, 2,3,4,5,6 = Signal Processing units, Others are either components or transformer input and output values.

can be ignored. This is because the inverter always maintains the operating point on the constant load line. Also we know that the output power of the MHD generator is a linear function of the fuel input rate and is related to the coal input rate W_{fuel} through a constant K. This means that the MHD generator-inverter can be represented as a linear element in the incremental power model of the combined plant.

2. INCREMENTAL POWER MODEL

To describe small changes about a steady state point, an incremental power model is constructed. The model is based on the incremental power behavior of the various plant components. The model is actually a linearized version of the plant behavior equations.

Considering the Laplace transforms of all power increments, the incremental power model for the combined plant is shown in Figure 8. A demand change $\Delta P_d(s)$ produces a frequency deviation $\Delta f(s)$ through the $K_4/(1 + \tau_4 s)$ block, where K_4 represents the effect of change in frequency due to the speed change of the rotating machinery in the system. For control $\Delta f(s)$ is sensed and is used to control the incremental fuel input rate $\Delta W_{fuel}(s)$.

K has already been calculated and is related to the gross calorific value of coal. K_0 represents the thermal process efficiency of the MHD combustor where the fuel is burnt. The combustor time constant τ_0 is related to the plasma residence

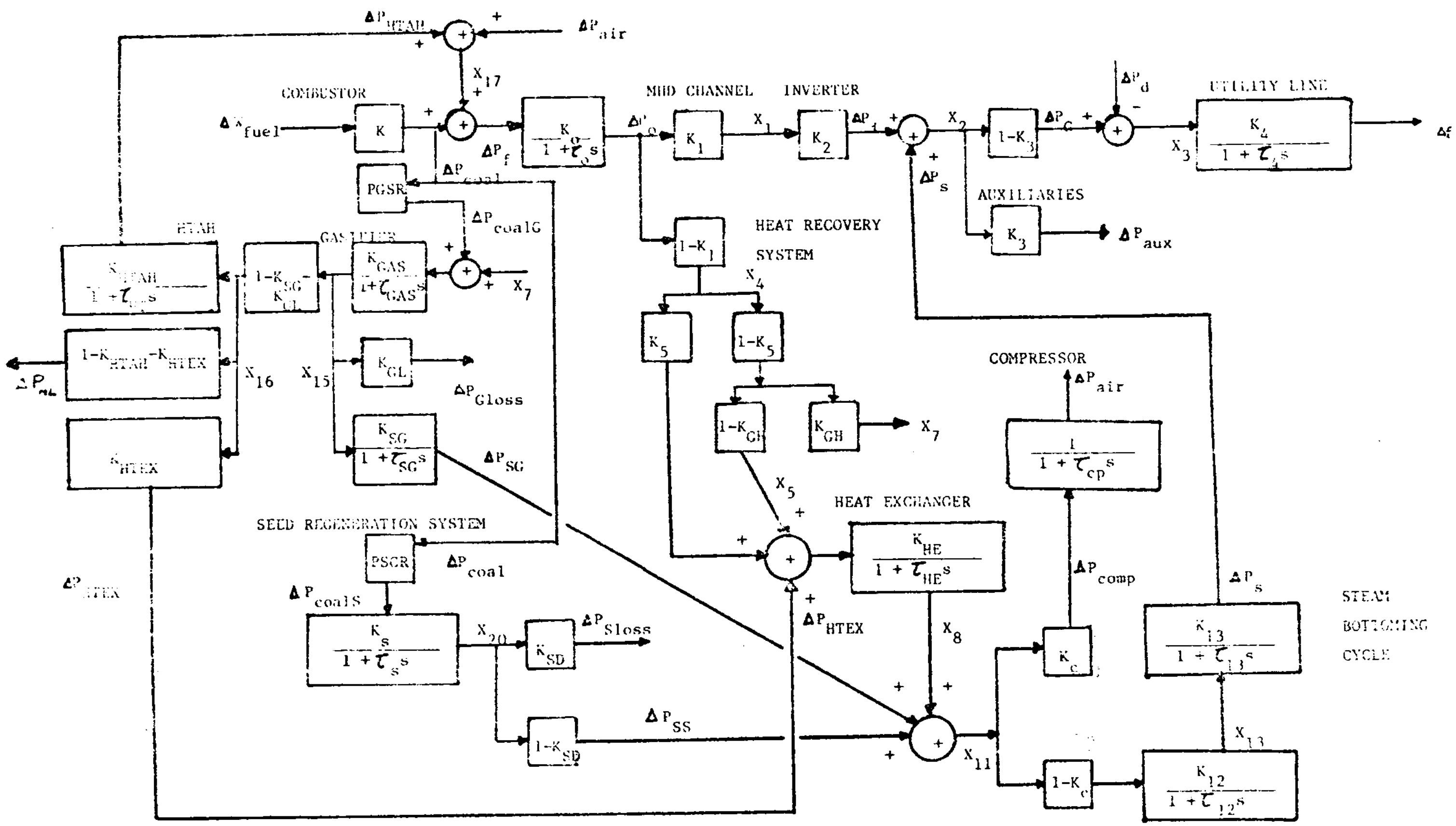

Figure 8. Incremental Power Model

time in the combustor. $\Delta P_{air}(s)$ is the change in the power in the preheated air being put in the combustor. $\Delta P_f(s)$ is the total change in the combustor power input which leads to the total change in the combustor output $\Delta P_0(s)$.

Blocks with gains K_1, K_2 and K_3 represent the effect of the changed load line on the inverter output $\Delta P_i(s)$ and the auxiliary power $\Delta P_{aux}(s)$. $X_3(s)$ is the power mismatch between the total change in power generation $\Delta P_G(s)$ and the change in power demand $\Delta P_d(s)$.

The diffuser, heat recovery system and air preheater are modeled by the blocks $(1 - K_1)$, $(1 - K_5)$ and $(1 - K_{GH})$ respectively. The blocks K_5 and K_{GH} represent the boiler feed water circulating in the diffuser and the air preheated for use in the gasifier. The rest of the heat goes into the heat exchanger modeled by the block $K_{HE}/(1 + \tau_{HE}s)$.

Steam is also produced in the gasifier $\Delta P_{SG}(s)$ and in the seed regeneration system $\Delta P_{SS}(s)$. The total steam thus available is $X_{11}(s)$ and is used in part to run the main compressor modeled by the blocks K_c and $1/(1 + \tau_{cp}s)$. The remaining superheated steam $X_{12}(s)$ runs a three stage turbine and an alternator. The net incremental power in the steam section is thus $\Delta P_s(s)$ which contributes to the total electric power produced $X_2(s)$.

The incremental models for the gasifier-HTAH and the seed regeneration system are linearized version of the actual models. The inputs to the gasifier change by amounts $\Delta P_{coalG}(s)$ and $X_7(s)$, being proportional to the change in the MHD channel input.

The entrained bed fluidizing coal gasifier is represented by the block $K_{GAS}/(1 + \tau_{GAS}s)$, where τ_{GAS} is related to the residence time in the gasifier. The gasifier produces some steam, the change being $\Delta P_{SG}(s)$. It is noted that the steam block $K_{SG}/(1 + \tau_{SG}s)$ has a much lower time constant than that of the main heat exchanger viz. $\tau_{HE} \gg \tau_{SG}$. Loss in the gasifier is modeled by a constant block K_{GL}. The clean gas produced by the gasifier is used to run the HTAH, which heat the air used in the MHD combustor. The heat change to air $\Delta P_{HTAH}(s)$ is determined by the block $K_{HTAH}/(1 + \tau_{HT}s)$. $\Delta P_{HTEX}(s)$ is the change in the exhaust gas heat and $\Delta P_{HTAHL}(s)$ is the change in the HTAH loss.

The seed regeneration system has a coal input $\Delta P_{coalS}(s)$ related to the fuel input to the MHD combustor. The furnace of this system is modeled by the first order block $K_s/(1 + \tau_s s)$ where τ_s is the time constant and is much lower than τ_{HE}. The change in the steam produced is $\Delta P_{SS}(s)$ and the heat loss change is $\Delta P_{sloss}(s)$.

3. A COMMERCIAL SCALE PLANT

Table 4 lists the representative values of various model parameters for a 1000 MW_e combined MHD/Steam plant. As seen in the table, most of the proportional constants are based on the steady state performance. The time constants for the various component blocks are based on the process dynamics of that particular component. The steam plant constants are based on existing literature. These parameters are sufficiently

TABLE 4

PARAMETER VALUES

Parameter	Value	Source
K	28.0 MW/kg/sec	Chapter 2
K_o	1.0	Steady State Model (SS)
K_1	0.22	SS
K_2	0.97	SS
K_3	0.05	SS
K_4	0.06	Machine Inertia
K_{GH}	0.08	SS
K_5	0.02	SS
K_{HE}	0.98	Heat Exchanger design
K_c	0.06	Compressor design
K_{12}	0.40	Turbine efficiency
K_{13}	0.98	Generator efficiency
K_{GAS}	0.98	SS
K_{SG}	0.10	Gasifier design
K_{GL}	0.01	Gasifier loss
K_{HTAH}	0.96	SS
K_{HTEX}	0.02	SS
K_s	1.0	SS
K_{SD}	0.36	SS
PSCR	0.12	SS
PGSR	0.55	Gasifier design
τ_o	0.05 second	MHD combustor design
τ_4	10.00 second	Steam generator lag
τ_{HE}	100.00 second	Reference (24)
τ_{12}	0.30 second	Reference (15)
τ_{13}	0.10 second	Reference (15)
τ_{GAS}	0.05 second	Gasifier design
τ_{SG}	10.00 second	Gasifier design
τ_{HT}	20.00 second	HTAH design
τ_{cp}	0.01 second	Compressor design
τ_s	0.05 second	Seed regeneration

accurate for control problems related to the combined plant.

The incremental power model with the parameter values as given in Table 4 was simulated on the IBM 370/65 computer using the Continous System Modelling Program (CSMP). In all the control techniques studied the change in power demand was a unit step of 10 MW_e, an increment of 1% over the steady state point. The CSMP program was used with the fourth order Runge-Kutta integration method with an integration step of 0.01 second. The computer time taken in a typical simulation program with a final integrating time of 100 seconds was found to be 1.0-1.5 minutes.

CHAPTER IV

CLASSICAL CONTROL

1. BACKGROUND

As has been shown before, the incremental coal input rate ΔW_{fuel} is the variable to be controlled by the frequency change Δf, so that the plant follows a change in load demand. The classical control functions considered here were of the following three types :

1. Integral (I)
2. Proportional-Integral (PI)
3. Proportional-Integral-Derivative (PID)

The integral control is necessary to attain a zero steady state error. A generalized PID feedback control scheme is shown in Figure 9. It is noted that only one variable is fed back in order to control the fuel input rate change.

2. PID CONTROL

Based on the results of Integral and Proportional-Integral controllers for various values of constants C_1 and C_2, the following values of these parameters were chosen to give the best performance in terms of minimum settling time, control effort and stability :

$C_1 = 20.0$

$C_2 = 10.0$

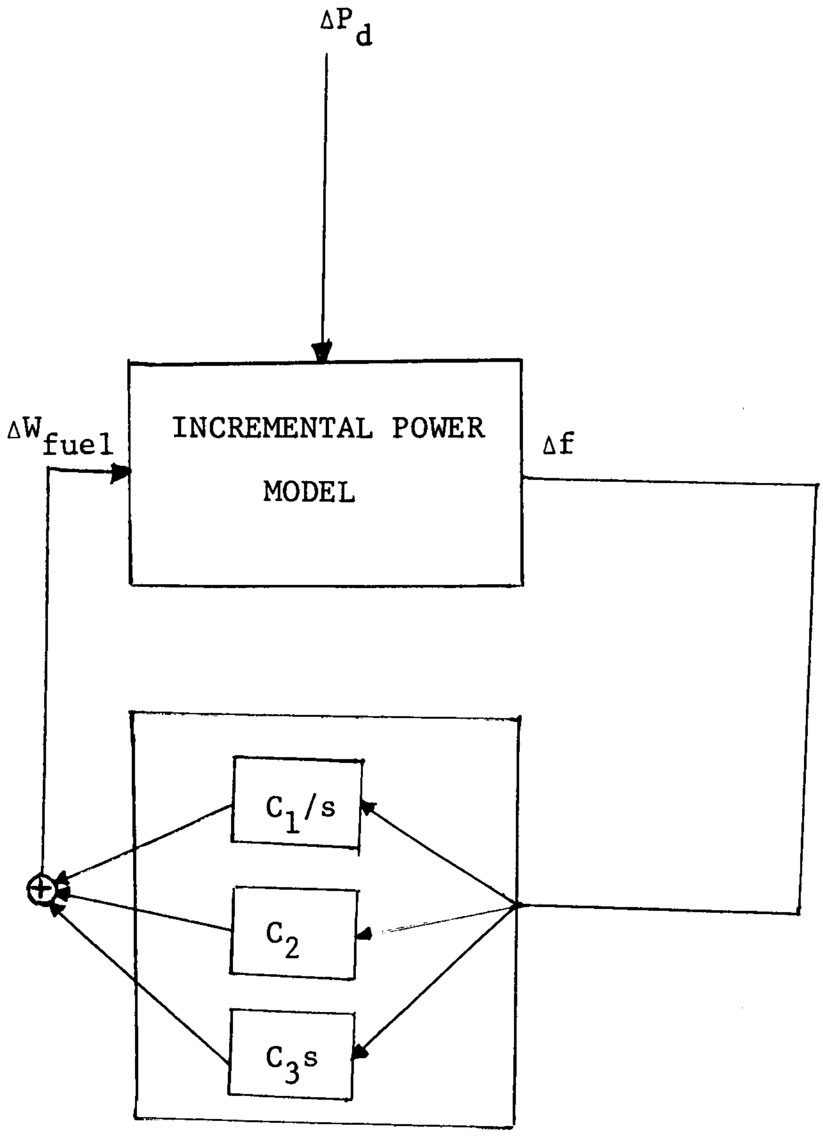

Figure 9. Generalized PID controller

To study the effect of a PID controller on the incremental power model, the following values of C_3 (the coefficient of the derivative feedback term) were used:

$C_3 = 1.0, 5.0, 10.0, 20.0$

The program incoporating the PID controller was written using the CSMP package (25,26). The variation of all the model variables with time was obtained and plotted. Figures 10 to 12 show some plots of interest. Figure 10 shows the frequency deviation for the cases of $C_3 = 1.0$, 5.0 and 10.0. Figure 11 shows the fuel input rate change variation with time and Figure 12 shows the power mismatch. In all three cases, the frequency deviation and power mismatch settle to zero eventually. The fuel input rate change settles to the new steady state value.

It is noted that the system settles down in 35-50 seconds based on a frequency tolerance of approximately 0.002 Hz. The steam section, however, takes a while before it starts producing maximum possible power output. This is due to a large heat exchanger time constant of 100 seconds. The MHD section is fast responding, thus resulting in a quick settling time. To get an idea of the load division during the transient period, ΔP_i - inverter output power change and ΔP_s - steam section output power change, are plotted in Figure 13 for the PID controller with a C_3 value of 10.0. The change in load demand, being 10 MW_e is not

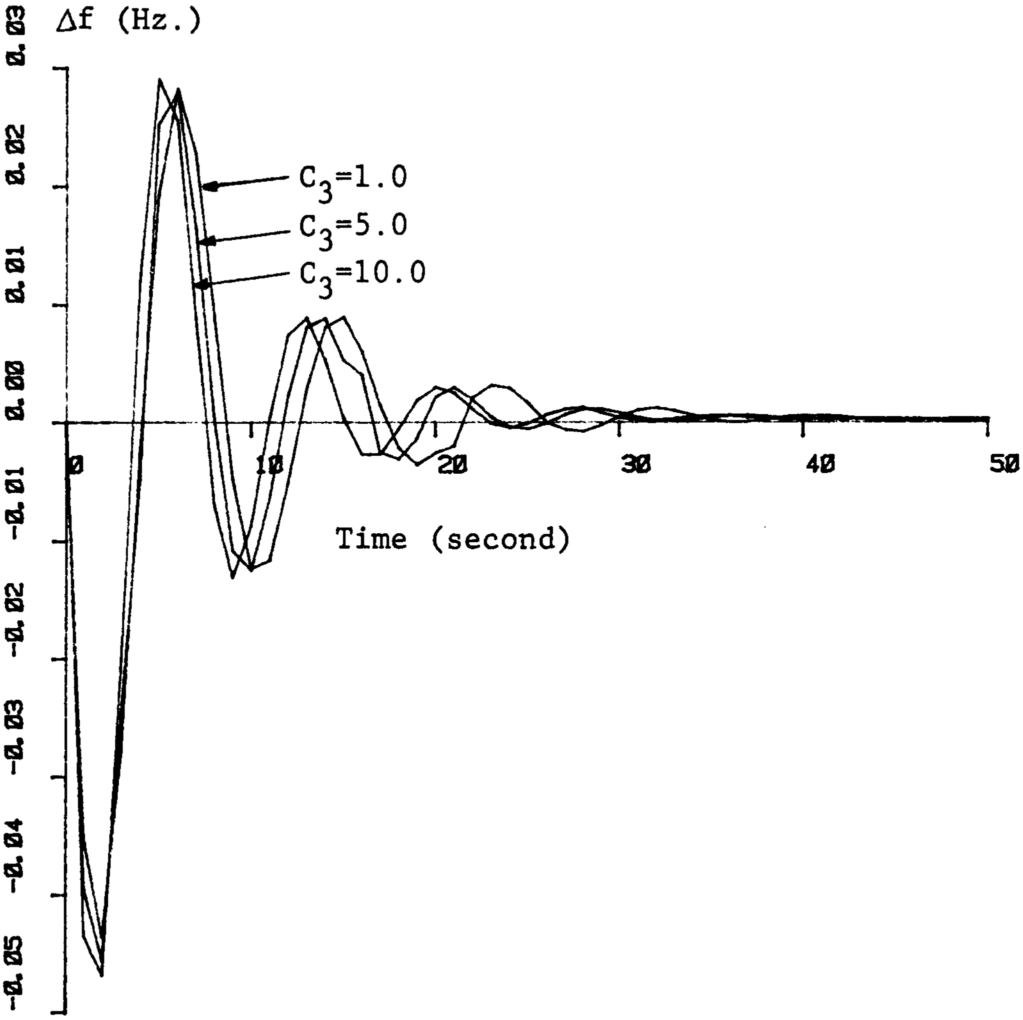

Figure 10. Frequency deviation for PID control

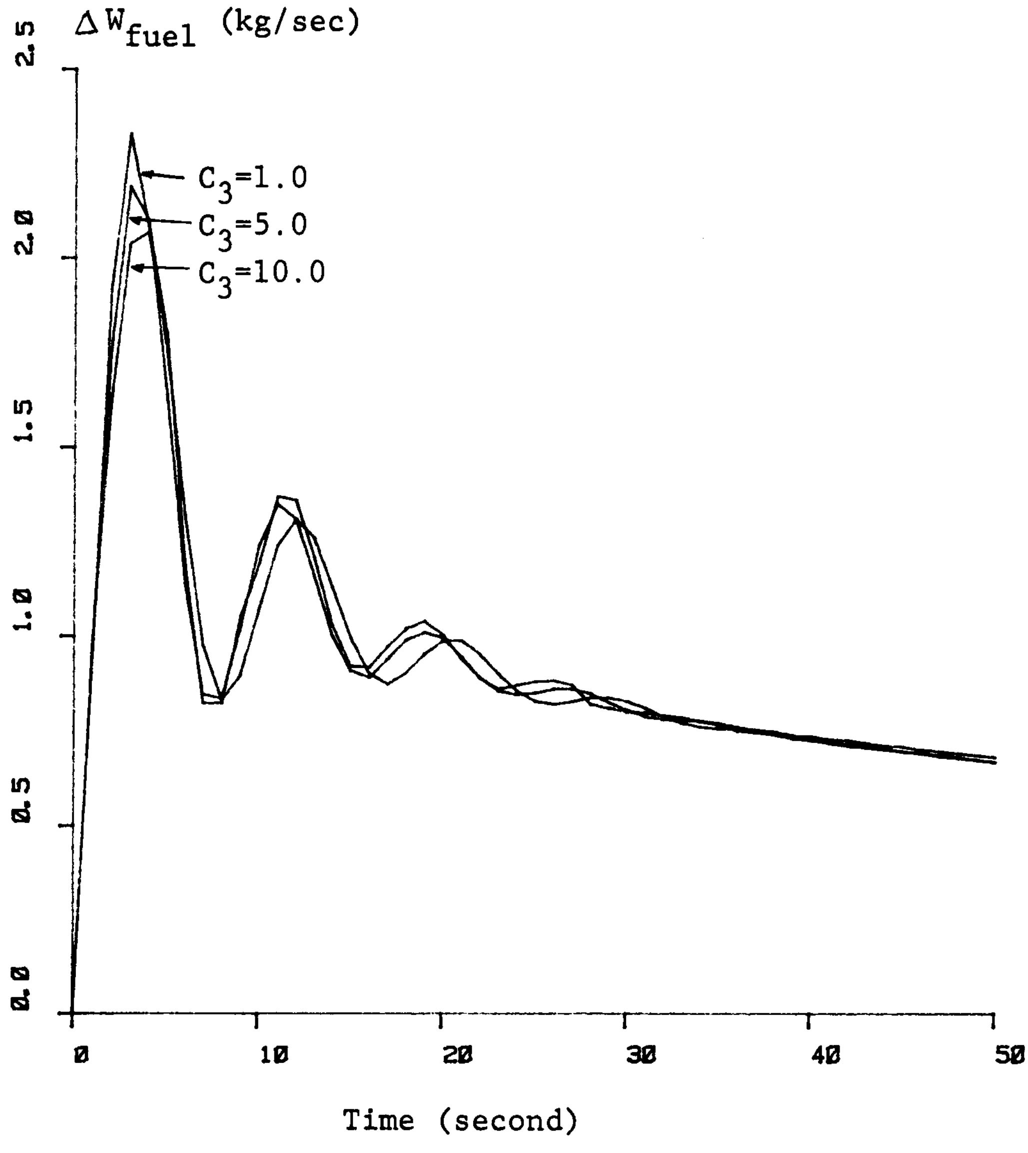

Figure 11. Fuel input rate change for PID control

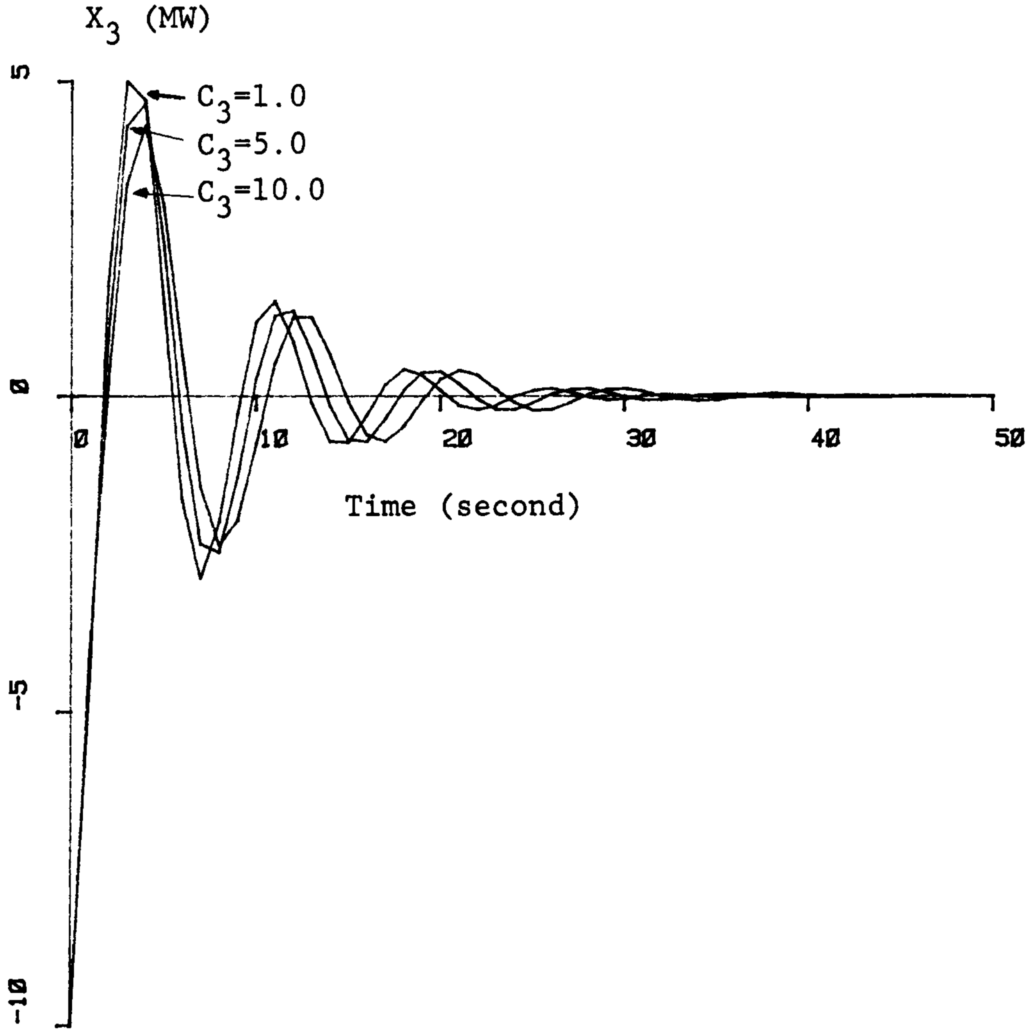

Figure 12. Power mismatch for PID control

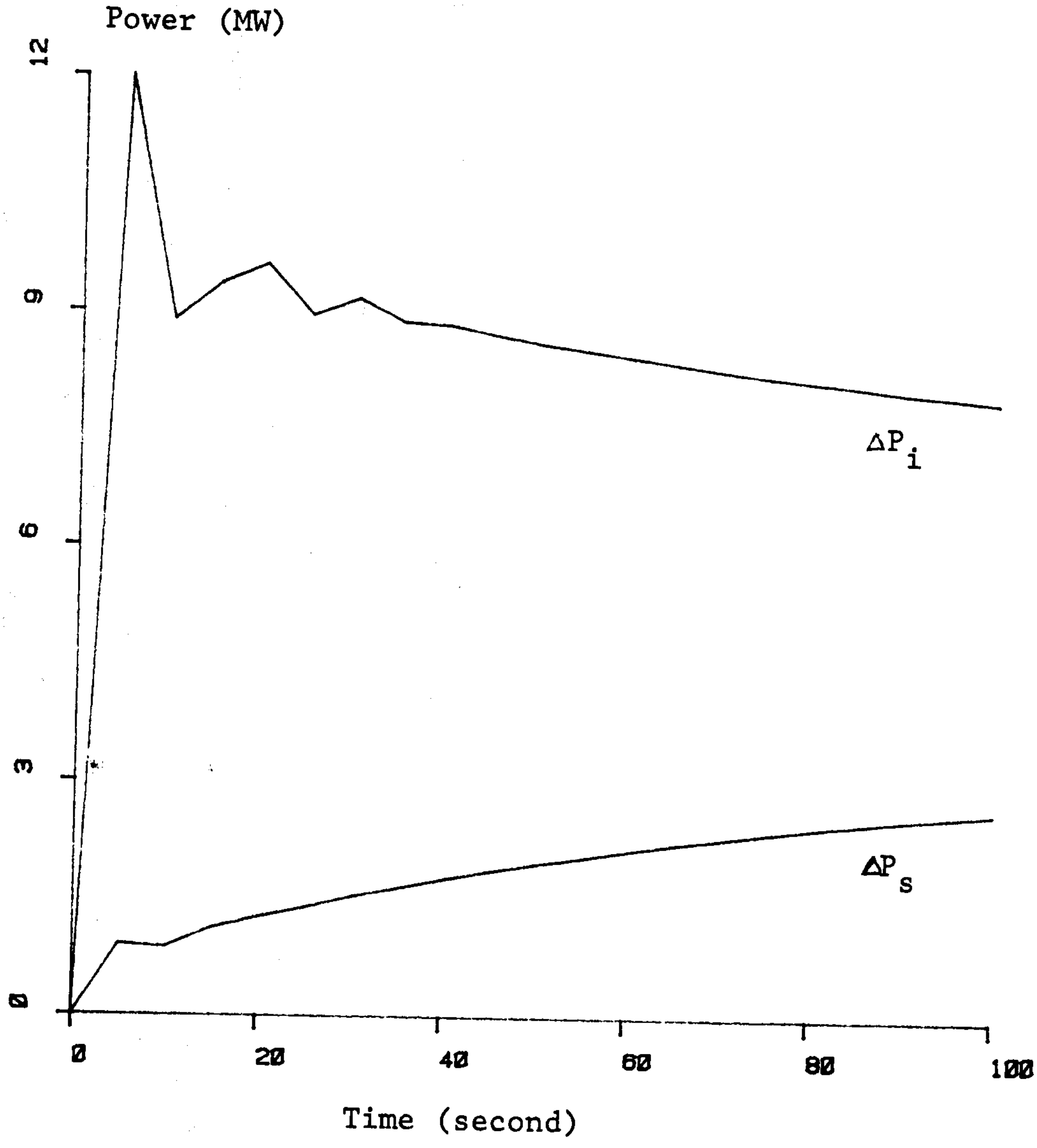

Figure 13. Load division for PID control
C_3=10.0

divided in the ratio of 40/60. This is due to the slow response of the steam plant.

3. RESULTS

Frequency error, Total control effort and Peak control effort were chosen as the criteria for the performance comparison of various control techniques. These parameters are defined below:

1. Frequency error in sec^{-1} is defined as

$$e_f = \int_0^\infty (\Delta f)^2 dt$$

It is a measure of frequency deviation during the transient period.

2. Total control effort in kg^2/sec is defined as

$$e_u = \int_0^\infty (\Delta W_{fuel})^2 dt$$

W_{fuel} is positive for all time $t>0$ for a ΔP_d step change. Total control effort, e_u is a measure of total change in coal input flow rate as the system settles down.

3. Peak control effort in kg/sec is defined as

$$p_u = \underset{0 \leq t < \infty}{\text{Maximum}} (\Delta W_{fuel})$$

It is a measure of peak change in fuel input rate. Since the plant is a realistic physical system, there is a maximum value of ΔW_{fuel} that the plant can handle. We consider 5% of the steady state value of W_{fuel} (54.4 kg/sec) to be this maximum for the case of ΔP_d being 10 MW_e. This means if a particular control scheme requires that the plant supply a ΔW_{fuel} of more than 2.72 kg/sec, then that scheme is not suitable.

The values of e_f, e_u and p_u for the various PID control schemes studied are listed in Table 5. The value of C_3=0.0 corresponds to only a PI controller and its performance is included for comparison purpose only. The values in Table 5 show that a PID controller is acceptable without any auxiliary boiler to speed up the response of the steam section. It is also noted that a value of C_3=10.0 in the PID control provides a reasonable peak control effort. This controller is chosen as being sufficient for our purpose. The total control effort for various cases is not a good criterion here for chosing a particular controller, since the variation in e_u is not significant.

TABLE 5

PID CONTROL PERFORMANCE

C_3	Frequency Error e_f $sec.^{-1}$	Total Control Effort, e_u $kg.^2sec^{-1}$	Peak Control Effort, p_u $kg.sec^{-1}$
0.0	6.81×10^{-3}	69.751	2.53
1.0	6.74×10^{-3}	67.846	2.33
5.0	6.53×10^{-3}	67.283	2.21
10.0	6.34×10^{-3}	66.785	2.10
20.0	6.09×10^{-3}	66.169	1.95

CHAPTER V

OPTIMAL CONTROL

The application of optimal control theory to the design of a control strategy involves representation of the system in a state variable form and the specification of a cost function.

1. PROBLEM FORMULATION

The dynamic behavior of a continous, linear, time invariant system is governed by an n-th order differential equation that relates the input and the output. The system is completely specified at any time t, provided n independent conditions define the state of the system at that time, the conditions be denoted by the vector $\underline{x}$ (27). The system can now be represented by the state variable differential equation given as

$$\dot{\underline{x}} = A\underline{x} + B\underline{u} \tag{5.1}$$

where

$\underline{x}$ n x 1 state vector

A n x n system matrix

$\underline{u}$ m x 1 input or control vector

B n x m input matrix

and the output y is given by the output equation

$$y = \underline{c}^T\underline{x} \tag{5.2}$$

where

$\underline{C}$ n x 1 output vector

The optimal control problem for this system requires the determination of a control input vector $\underline{u}$ which minimizes the cost function (28)

$$J = \frac{1}{2}\int_0^\infty (\underline{x}^T Q \underline{x} + \underline{u}^T R \underline{u})dt \qquad (5.3)$$

where

Q   n x n positive semidefinite symmetric state cost weighting matrix

R   m x m positive definite symmetric input cost weighting matrix

2. PROBLEM SOLUTION

J represents the cost that is to be minimized by the optimal controller for the system. R and Q matricies weigh the input control effort and the system state variables in the optimal control problem.

The optimal control that minimizes the cost of the system is a function of the present state of the system

$$\underline{u} = - K\underline{x} \qquad (5.4)$$

where

$$K = R^{-1}B^TP$$

K being a m x n matrix and P being the symmetric and positive definite solution of the algebraic matrix Riccati equation (28)

$$PA - PBR^{-1}B^TP + A^TP + Q = 0 \qquad (5.5)$$

This control strategy is also termed as 'State variable feedback control', since $\underline{u}$ is a function of all the state variables. The following conditions must be satisfied for a optimal controller design (29):

1. The pair (A,B) must be completely controllable.

2. The pair (A,D) must be completely observable, where D is a n x n matrix such that $DD^T = Q$.

3. OPTIMAL CONTROL OF THE INCREMENTAL POWER MODEL

From the incremental power model of the commercial scale MHD/Steam plant, eight state variables are recognized,

$$\underline{x} = \left[\Delta f \;\; \Delta P_o \;\; \Delta P_{air} \;\; \Delta P_s \;\; \Delta P_{HTAH} \;\; X_{11} \;\; X_{13} \;\; X_{15}\right]^T$$

ΔP_{SG} and X_{20} are not included since τ_{HE} is much greater than τ_s and τ_{SG}, so that the corresponding first order blocks can be approximated as constants ($\Delta P_{SG} = K_{SG}X_{15}$ and $X_{20} = K_s \Delta P_{coalS}$). The system equation becomes

$$\dot{\underline{x}} = A\underline{x} + \underline{B}\,\Delta W_{fuel} + \underline{F}\,\Delta P_d \qquad (5.6)$$

where

$$A = \begin{bmatrix} -1/\tau_4 & A_{12} & 0 & A_{14} & 0 & 0 & 0 & 0 \\ 0 & -1/\tau_o & K_o/\tau_o & 0 & 0 & 0 & 0 & 0 \\ 0 & 0 & -1/\tau_{cp} & 0 & 1/\tau_{cp} & K_c/\tau_{cp} & 0 & 0 \\ 0 & 0 & 0 & -1/\tau_{13} & 0 & K_{13}/\tau_{13} & 0 & 0 \\ 0 & 0 & 0 & 0 & -1/\tau_{HT} & 0 & 0 & A_{58} \\ 0 & A_{62} & 0 & 0 & 0 & -1/\tau_{HE} & 0 & A_{68} \\ 0 & 0 & 0 & 0 & 0 & A_{76} & -1/\tau_{12} & 0 \\ 0 & A_{82} & 0 & 0 & 0 & 0 & 0 & -1/\tau_{GAS} \end{bmatrix}$$

$\underline{F} = [-K_4/\tau_4 \quad 0 \quad 0 \quad 0 \quad 0 \quad 0 \quad 0 \quad 0]^T$

$\underline{B} = [\ 0 \quad KK_o/\tau_o \quad 0 \quad 0 \quad 0 \quad b_6 \quad 0 \quad b_8]^T$

$A_{12} = K_1K_2(1 - K_3)K_4/\tau_4$

$A_{14} = (1 - K_3)K_4/\tau_4$

$A_{58} = (1 - K_{SG} - K_{GL})K_{HTAH}/\tau_{HT}$

$A_{62} = K_{HE}(K_5(1 - K_1) + (1 - K_5)(1 - K_1)(1 - K_{GH}))/\tau_{HE}$

$A_{68} = (K_{SG}/\tau_{SG} + K_{HE}K_{HTEX}(1 - K_{SG} - K_{GL})/\tau_{HE})$

$A_{76} = K_{12}(1 - K_c)/\tau_{12}$

$A_{82} = K_{GAS}K_{GH}(1 - K_5)(1 - K_1)/\tau_{GAS}$

$b_6 = (1 - K_{SD})K_sK.PSCR/\tau_{SD}$

$b_8 = K_{GAS}K.PGSR/\tau_{GAS}$

Based on the representative values of the various parameters from Table 4, the system equation for the incremental power model takes the form

$$\dot{\underline{x}} = \begin{bmatrix} -0.1 & 0.0012 & 0 & 0.0056 & 0 & 0 & 0 & 0 \\ 0 & -20.0 & -20.0 & 0 & 0 & 0 & 0 & 0 \\ 0 & 0 & -100 & 0 & 100 & 6.6 & 0 & 0 \\ 0 & 0 & 0 & -10.0 & 0 & 9.8 & 0 & 0 \\ 0 & 0 & 0 & 0 & -.05 & 0 & 0 & .043 \\ 0 & .007 & 0 & 0 & 0 & -.1 & 0 & .099 \\ 0 & 0 & 0 & 0 & 0 & 1.2 & -3.3 & 0 \\ 0 & 1.26 & 0 & 0 & 0 & 0 & 0 & -20 \end{bmatrix} \underline{x} +$$

$$[0 \quad 560 \quad 0 \quad 0 \quad 0 \quad 44.4 \quad 0 \quad 304.3]^T \Delta W_{fuel} +$$

$$[-.006 \quad 0 \quad 0 \quad 0 \quad 0 \quad 0 \quad 0 \quad 0]^T \Delta P_d \qquad (5.7)$$

This model equation contains an independent input $\underline{F}\Delta P_d$ which is not present in equation (5.1). To apply optimal control theory, the states are redefined in terms of their steady state values, i.e.

$$\underline{x}' = \underline{x} - \underline{x}_{ss} \tag{5.8}$$

In order to determine the steady state vector $\underline{x}_{ss}$, the equation (5.7) is put to zero

$$\dot{\underline{x}}_{ss} = A\underline{x}_{ss} + \underline{B}\Delta W_{fuelss} + \underline{F}\Delta P_d = o \tag{5.9}$$

where ΔP_d will be considered to a step input. Since the steady state ferquency deviation is required to be zero, this leads to the following solution in terms of ΔP_d

$$\begin{aligned}
\Delta f_{ss} &= 0 \\
\Delta P_{oss} &= 2.06\Delta P_d \\
\Delta P_{airss} &= 0.747\Delta P_d \\
\Delta P_{sss} &= 0.60\Delta P_d \\
\Delta P_{HTAHss} &= 0.64\Delta P_d \\
X_{11ss} &= 1.64\Delta P_d \\
X_{13ss} &= 0.613\Delta P_d \\
X_{15ss} &= 0.748\Delta P_d \\
\Delta W_{fuelss} &= 0.0492\Delta P_d
\end{aligned} \tag{5.10}$$

This change in variables puts equation (5.7) in the form

$$\dot{\underline{x}}' = A\underline{x}' + \underline{B}\Delta W_{fuel}' \tag{5.11}$$

where

$$\underline{x}'(0) = -\underline{x}_{ss}$$

$$\Delta W_{fuel}'(0) = -\Delta W_{fuelss}$$

A and $\underline{B}$ remain the same as before. The cost J is constructed using R = 1 and

$$Q = \begin{bmatrix} \alpha & 0 & 0 & 0 & 0 & 0 & 0 & 0 \\ 0 & 0 & 0 & 0 & 0 & 0 & 0 & 0 \\ 0 & 0 & 0 & 0 & 0 & 0 & 0 & 0 \\ 0 & 0 & 0 & 0 & 0 & 0 & 0 & 0 \\ 0 & 0 & 0 & 0 & 0 & 0 & 0 & 0 \\ 0 & 0 & 0 & 0 & 0 & 0 & 0 & 0 \\ 0 & 0 & 0 & 0 & 0 & 0 & 0 & 0 \\ 0 & 0 & 0 & 0 & 0 & 0 & 0 & 0 \end{bmatrix} \tag{5.12}$$

such that,

$$J = \frac{1}{2}\int_0^\infty (\alpha\Delta f'^2 + \Delta W_{fuel}'^2)dt \tag{5.13}$$

Here $\alpha(\Delta f')^2$ restricts the frequency deviation, while $(\Delta W_{fuel}')^2$ penalizes the control effort needed in addition to the steady state value of the fuel input rate change.

4. RESULTS

The Riccati equation (5.5) was solved on an IBM 370/65 computer for α varying between 100 and 15000. The program checks for the controllability of the matrix pair (A,B) and for the observability of the pair (A,D) and then computes P. Based on the matrix P, $\Delta W_{fuel}'$ is evaluated as a linear combination of the state variable vector components as,

$$\begin{aligned} \Delta W_{fuel}' &= \Delta W_{fuel} - \Delta W_{fuelss} \\ &= [C_{11} \quad C_{12} \quad \cdots \quad C_{18}]\, \underline{x}' \end{aligned} \tag{5.14}$$

The coefficients C_{11} to C_{18} for the various values of α

are listed in Table 6. It is noted that the value of all the coefficients increase with the increase in α. The value of C_{17} is found to be zero in all cases. This is due to a low value of τ_{12}.

The system together with the optimal controller was simulated using the CSMP package, for various cases of α. The frequency response, fuel input rate variation and power mismatch curves for a number of cases of interest were plotted in Figures 14 to 16. The system in most cases settles to a new steady state in 40-60 seconds. The load division between the MHD and the steam section is illustrated for the case of α= 1000 in Figure 17.

Compared to the PID controller, the settling time is almost equal in all the cases considered. The total frequency error, total control effort and peak control effort will be compared in the next section. The load division appears to approach the new steady state value faster than for a single feedback PID controller.

5. DISCUSSION

The values obtained for e_f, e_u and p_u using optimal control are listed in Table 7. The frequency deviation error decreases while the total control effort increases with the increase in the value of α. This is expected since α is the weight on the frequency deviation in the cost function. The

TABLE 6

OPTIMAL CONTROL FEEDBACK COEFFICIENTS

α	C_{11}	C_{12}	C_{13}	C_{14}	C_{15}	C_{16}	C_{17}	C_{18}
100	9.18	.00057	.00011	.0051	.0092	.0408	0.0	.00003
500	21.15	.00128	.00025	.0114	.0131	.0568	0.0	.00005
1000	30.20	.00181	.00036	.0160	.0151	.0644	0.0	.00005
2000	43.05	.00255	.00050	.0221	.0172	.0723	0.0	.00006
5000	68.65	.00398	.00078	.0337	.0201	.0824	0.0	.00006
10000	97.61	.00554	.00108	.0457	.0223	.0893	0.0	.00007
15000	119.87	.00669	.00131	.0543	.0236	.0925	0.0	.00007

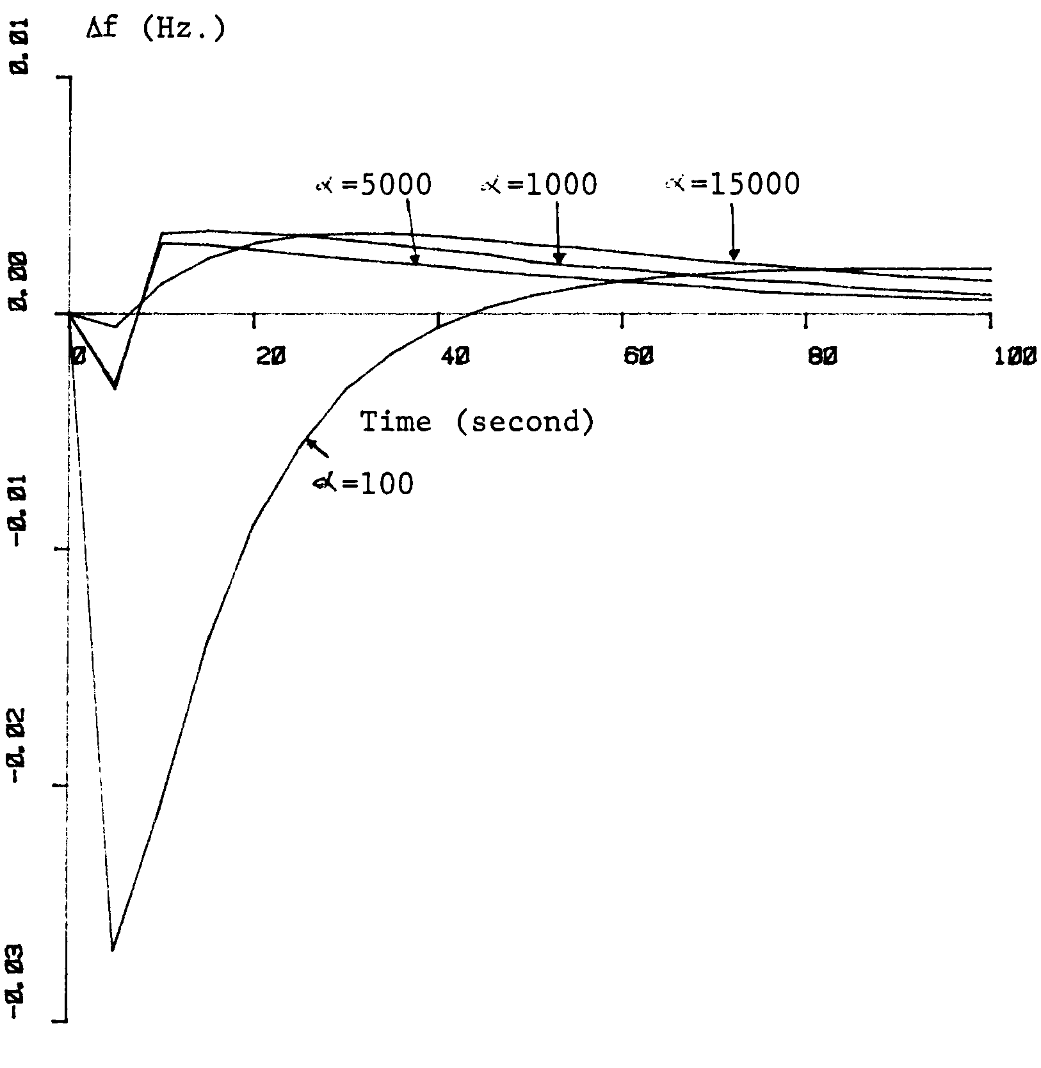

Figure 14. Frequency deviation for optimal control

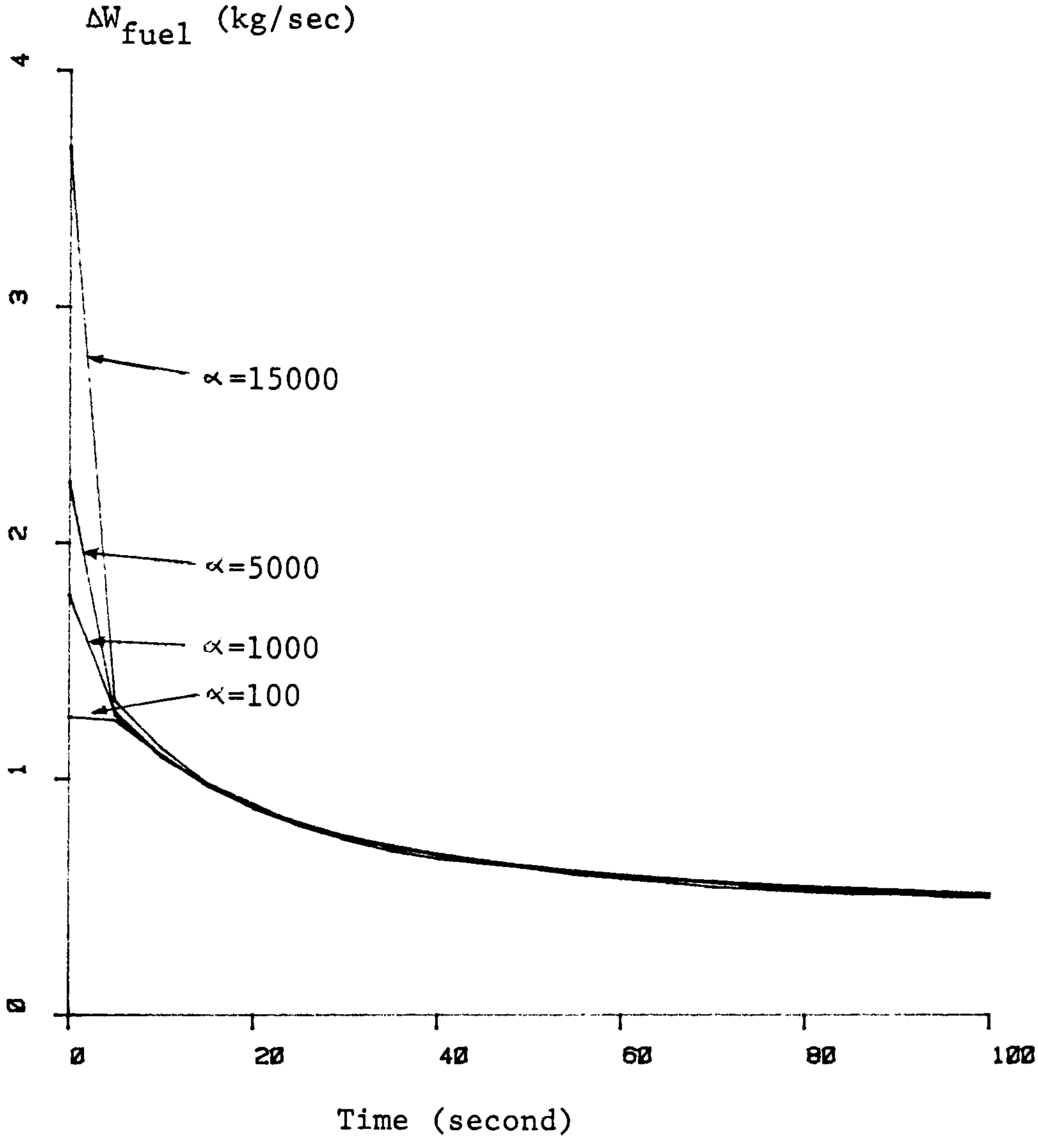

Figure 15. Fuel input rate change for optimal control

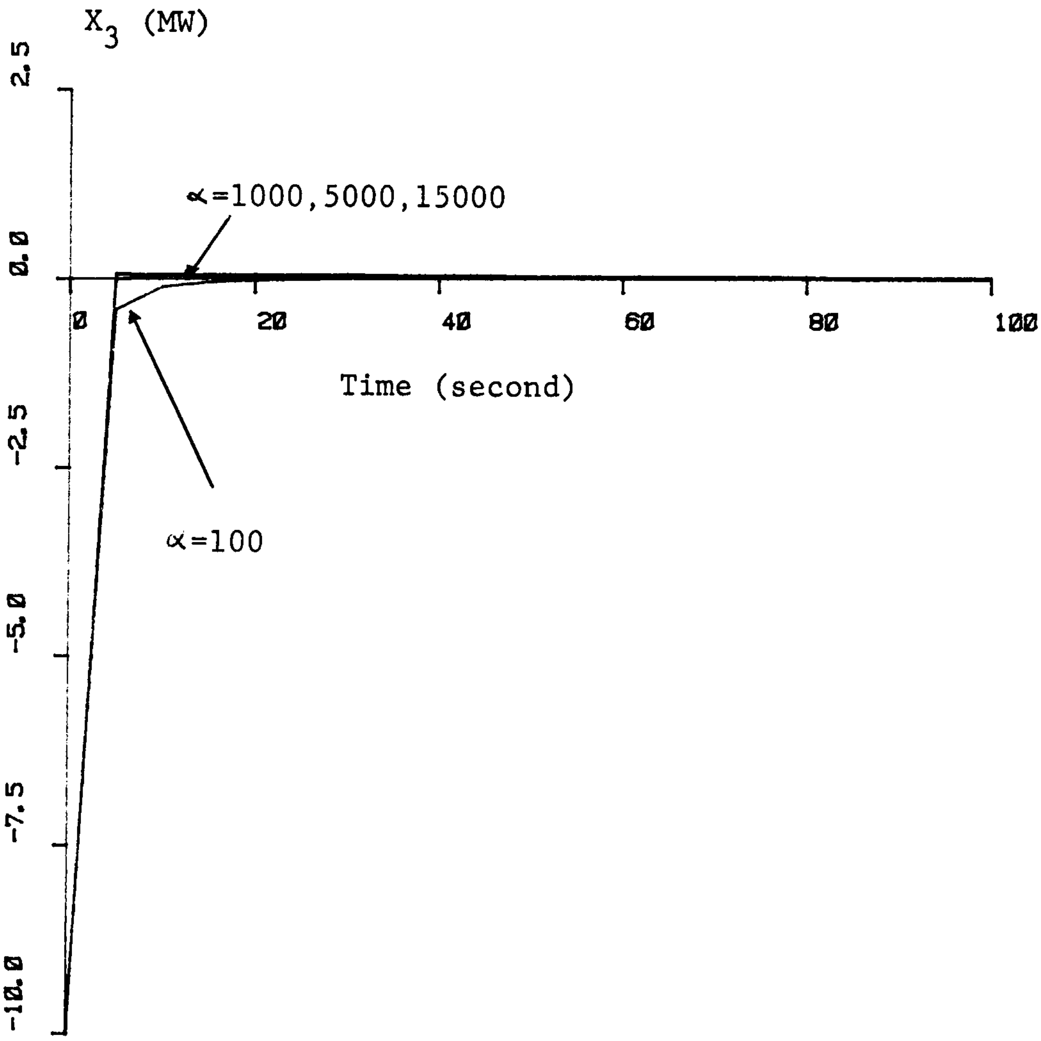

Figure 16. Power mismatch for optimal control

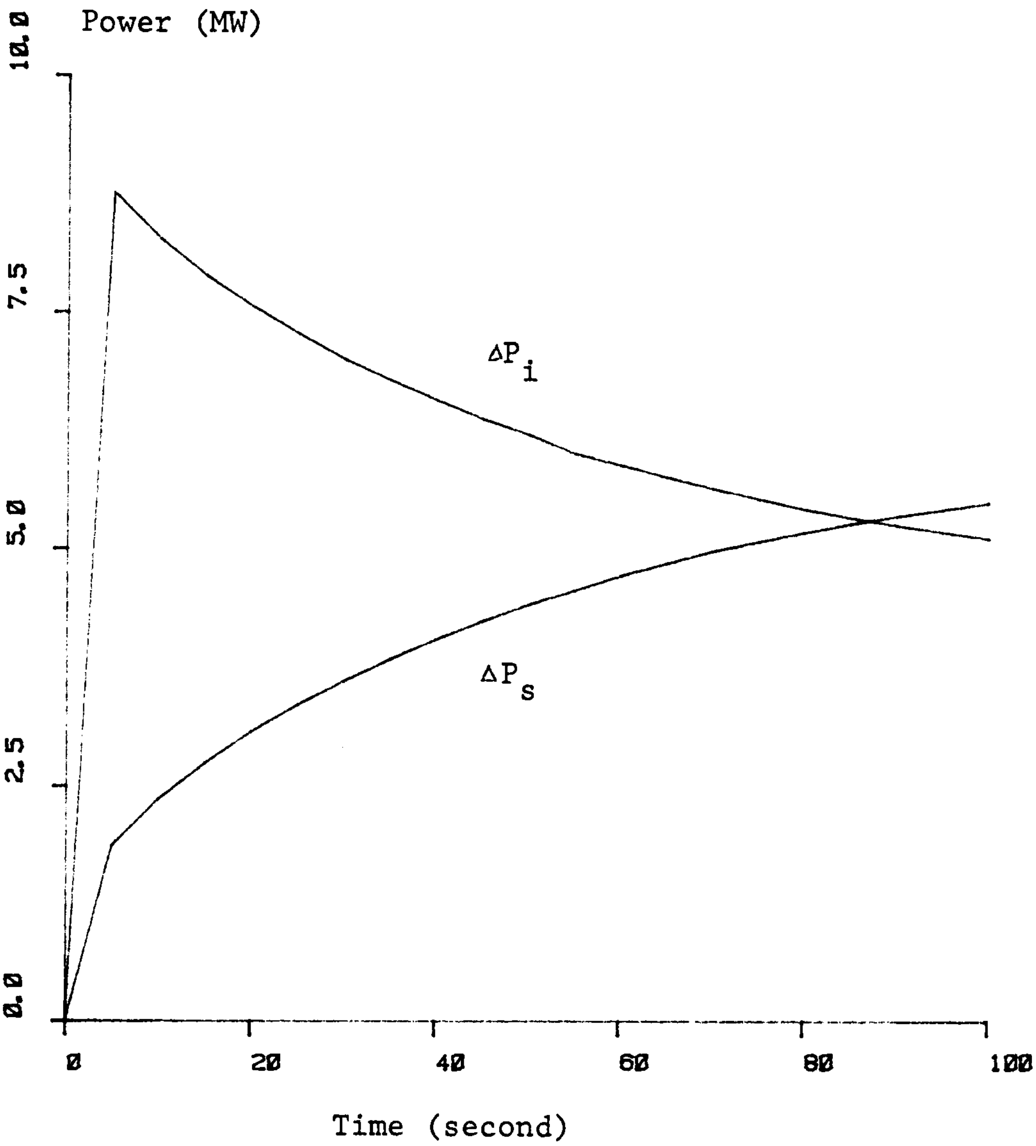

Figure 17. Load division for optimal control α=1000

TABLE 7

OPTIMAL CONTROL PERFORMANCE

α	Frequency Error e_f sec.$^{-1}$	Total Control Effort, e_u kg.^{2}sec^{-1}	Peak Control Effort, p_u kg.sec^{-1}
100	8.40×10^{-3}	56.15	1.28
500	7.82×10^{-4}	57.71	1.60
1000	6.38×10^{-4}	58.01	1.78
2000	6.06×10^{-4}	58.17	1.98
5000	5.85×10^{-4}	58.38	2.26
10000	4.60×10^{-4}	58.56	2.43
15000	3.80×10^{-4}	58.81	2.69

peak control effort increases as α is increased. For the value of α greater than 15000, p_u becomes more than 2.72 kg/sec. Thus a value of α more than 15000 should not be chosen. The variation in total control effort is not very significant in the cases considered. However frequency error and peak control effort can be used as two criteria to chose the most suitable optimal controller. Based on these criteria, α of 1000 is quite acceptable since it provides a set of reasonable values of e_f, e_u and p_u.

The values of e_f, e_u and p_u in most cases are smaller than for a single feeback PID controller (Table 5, page 38). It be kept in mind here that the state variable control does, however, require that each state variable be made available, either by direct measurement or by the construction of an observer (29). It has been verified that for the combined plant it is possible to measure directly or indirectly the values of all the state variables at any given time.

It is concluded that the state variable feedback yields an overall better system response than that given by the PID control scheme. The optimal controller does not require any storage for integrals and derivatives and requires computation of only one number at a time. It is recommended that since the difference in performance is not very large, the choice of using any particular controller be based on the ease of implementation, operation, reliability and maintainence.

CHAPTER VI

DIGITAL CONTROL TECHNIQUES

Recently computers have been used as control elements in many industrial applications. Such systems may be treated as sampled-data systems, since the information fed into the digital computer is the corresponding signal value only at one instant of time. The computed output remains unchanged until new information at the next sampling instant is fed into the computer.

1. SYSTEM CONDITIONS

Since we are interested in dedicated microprocessor based digital controllers which are in turn controlled by a digital computer, these goals place stringent conditions on the control algorithm that can be used. The conditions are (30):

1. The parameters of the process model must be directly related to easily measurable and easily computed process quantities.

2. The on-line control computation must be simple enough to carry out within the sampling period available.

3. It must be possible to compute the controller outputs from the process model parameters without carrying out any iterations. This requires that no integrations or derivatives be required to be evaluated for control output computation.

2. DISCRETE SYSTEM MODEL

For the application of digital control, we represent the incremental power model in the discrete form as

$$\underline{x}(\overline{m+1}\ T) = A_d\underline{x}(mT) + \underline{h}(T)u(mT) \qquad (6.1)$$

where

A_d n x n system matrix

$\underline{h}$ n x 1 control vector

u control input equal to ΔW_{fuel}'

$\underline{x}$ state variable vector equal to $\underline{x}'$

T sampling interval or period

The value of $\underline{x}$ at discrete time intervals is governed by this equation. The system is controllable if the set of matrices $A_d^{-1}\underline{h}$, $A_d^{-2}\underline{h}$ ... $A_d^{-n}\underline{h}$ are linearly independent (27). If this is the case, a time optimal control algorithm can be applied for driving $\underline{x}$ to a desired point in n time intervals, for a system with n state variables. We will apply one such control algorithm to a discrete model of the combined plant.

3. FINITE-TIME SETTLING CONTROL ALGORITHM

Figure 18 shows a schematic of a digital controller applied to a continous time system. The input to the plant is sampled and is held constant over each interval. This particular procedure is more satisfactory than the continous control, since here the control effort is piecewise continous and can be easily generated.

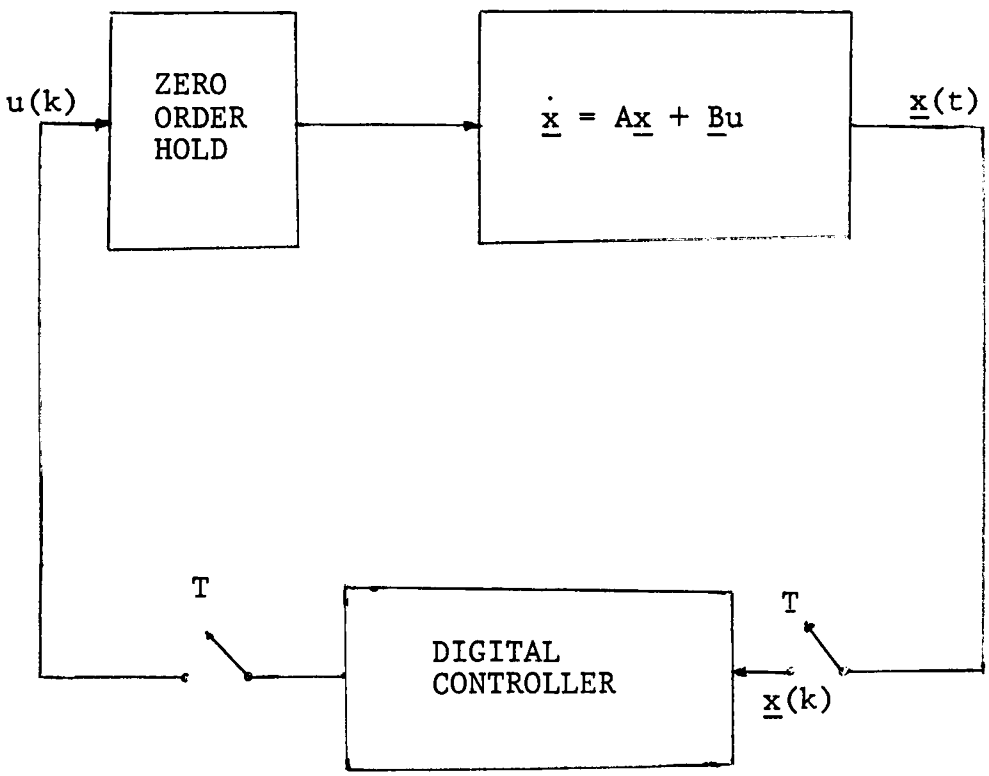

Figure 18. Schematic of a digital controller

It can be shown (27,31) that if the input is sampled, then we have

$$\underline{x}(0) = -M\underline{u} \tag{6.2}$$

or

$$\underline{u} = [\,u(0)\ u(1)\ \dots\ u(n-1)\,]^T = -M^{-1}\underline{x}(0) \tag{6.3}$$

where

$$M = [\,A_d^{-1}\underline{h}\ \ A_d^{-2}\underline{h}\ \ \dots\ \ A_d^{-n}\underline{h}\,] \tag{6.4}$$

This input gives control at each step to drive $\underline{x}(n)$ to zero. Here n refers to the n time interval. This control gives the value of u(k), k = 0, 1, 2, ... n-1 in terms of the values $\underline{x}(0)$. It would be more reliable if a given u(k) could be found in terms of just $\underline{x}(k)$ at the start of each sampling period. This helps in removing the effect due to external noise in the measuring devices. It is desirable to have u(k) as a constant linear combination of the state variables $\underline{x}(k)$.

The Finite-Time settling algorithm is based on the two conditions:

$$\begin{aligned} \underline{x}(n) &= \underline{0} \\ \underline{x}(0) &= -M\underline{u}(0) \end{aligned} \tag{6.5}$$

Applying these conditions to the discrete equation form (6.1) we obtain,

$$\begin{aligned} \underline{x}(1) &= A_d\underline{x}(0) + \underline{h}u(0) \\ &= -M\,[u(1)\ u(2)\ \dots\ u(n-1)\ 0]^T \end{aligned} \tag{6.6}$$

and

$$\begin{aligned} \underline{x}(2) &= A_d\underline{x}(1) + \underline{h}u(1) \\ &= -M\,[u(2)\ u(3)\ \dots\ u(n-1)\ 0\ 0]^T \end{aligned} \tag{6.7}$$

In general we have,

$$\underline{x}(k) = -M \left[u(k)\ u(k+1)\ \ldots\ u(n-1)\ 0\ \ldots\ 0 \right]^T \quad (6.8)$$

down to the equation for $\underline{x}(n-1)$ as

$$\underline{x}(n-1) = -M \left[u(n-1)\ 0\ 0\ \ldots\ 0 \right]^T \quad (6.9)$$

Now we can put $\underline{x}(k)$ as column of a matrix such that,

$$\left[\underline{x}(0)\quad \underline{x}(1)\quad \ldots\quad \underline{x}(n-1) \right] = -M.U \quad (6.10)$$

where the first row of matrix U is the control function we want. We therefore have,

$$\begin{aligned} X &= -M.U \\ U &= -M^{-1}.X \end{aligned} \quad (6.11)$$

Thus we can find U if M is non-singular i.e. the system is controllable. Then u(k) is a linear combination of the state variables $\underline{x}(k)$. This combination is given by first row of matrix $-M^{-1}$.

4. DIGITAL CONTROL OF THE MHD/STEAM PLANT

The Finite-Time settling control algorithm (FTSC) can now be applied to the incremental power model. A discrete representation of the form (6.1) is found for various values of sampling interval T. The procedure for calculating A_d and $\underline{h}(T)$ is described in detail in reference (27). The basic formulae are

$$\begin{aligned} A_d &= \exp(AT) \\ \underline{h} &= \int_0^{\tau} \exp(A\tau)\underline{b}.d\tau \end{aligned} \quad (6.12)$$

A_d and $\underline{h}$ are functions of T which was allowed to take the values of 0.1, 1.0, 2.0 and 5.0 seconds. The system is of order 8, thus 8T seconds are required to drive the system to the new steady state i.e. to go from $\underline{x}'(0)$ to $\underline{0}$.

A computer program was written to calculate A_d and $\underline{h}$ and check if the system is fully controllable. Then the state variable feedback coefficients are computed based on the first row of matrix $-M^{-1}$. It was found that the peak control effort for the case of T = 0.1 second was very high compared to the 2.72 kg/sec limit. Thus it was not considered further. For the other values of T, the frequency response, fuel input rate change and power mismatch were obtained as a function of time and are plotted in Figures 19 to 21.

It is noted that the system settles to a new steady state in 10-50 seconds depending on the sampling interval. The variation in Δf and ΔW_{fuel} is larger than for the PID and optimal controllers. This is because the system settles to a new steady state very fast and thus considerable control effort is necessary to accomplish this. The load division is of interest here. The load division between the MHD and steam section is shown in Figure 22. The case chosen is for T = 5 seconds. It is seen that the ΔP_i and ΔP_s both reach the new steady state value in about 50 seconds. This is expected since all the state variables are driven to the new value in approximately 8T seconds. The load division response is faster than any other types of controllers considered before.

5. DISCUSSION

The values for e_f, e_u and p_u are listed in Table 8. The frequency error and the total control effort both decrease with

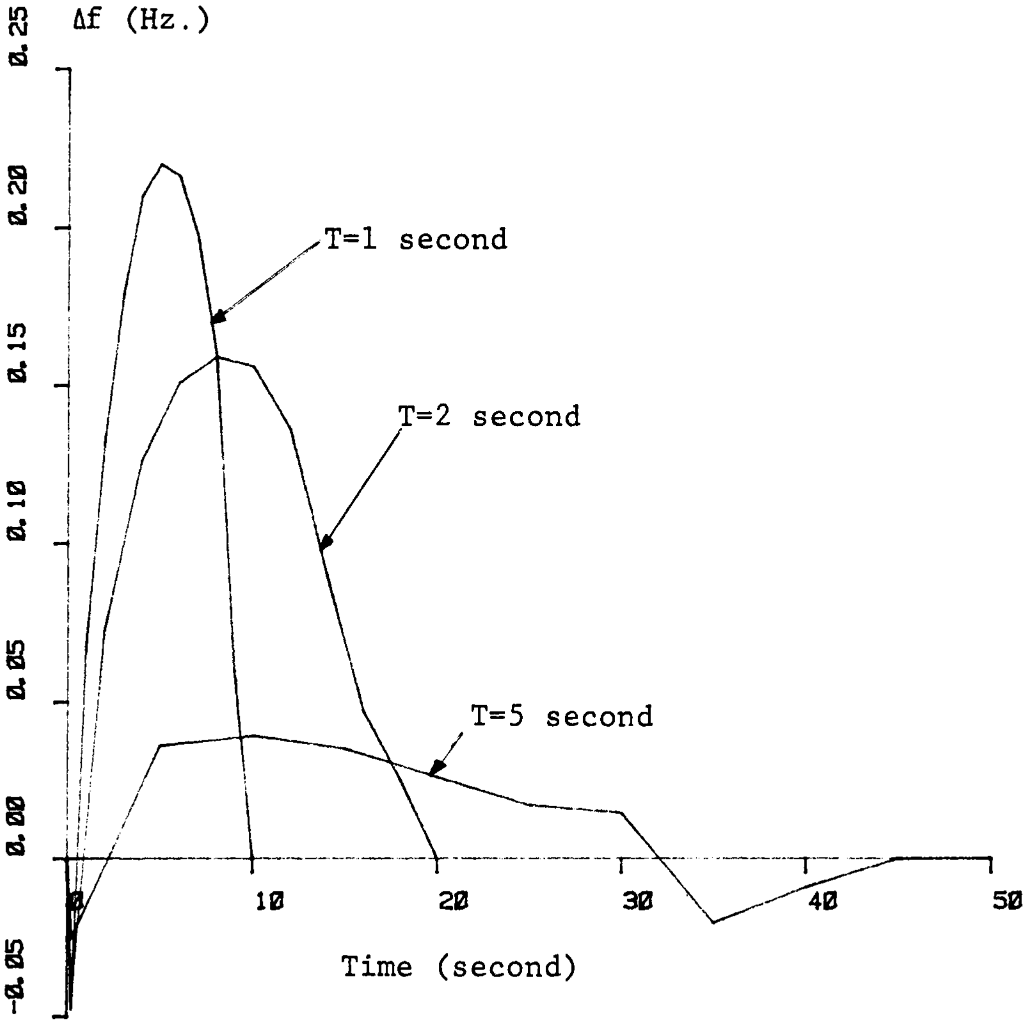

Figure 19. Frequency deviation for digital control

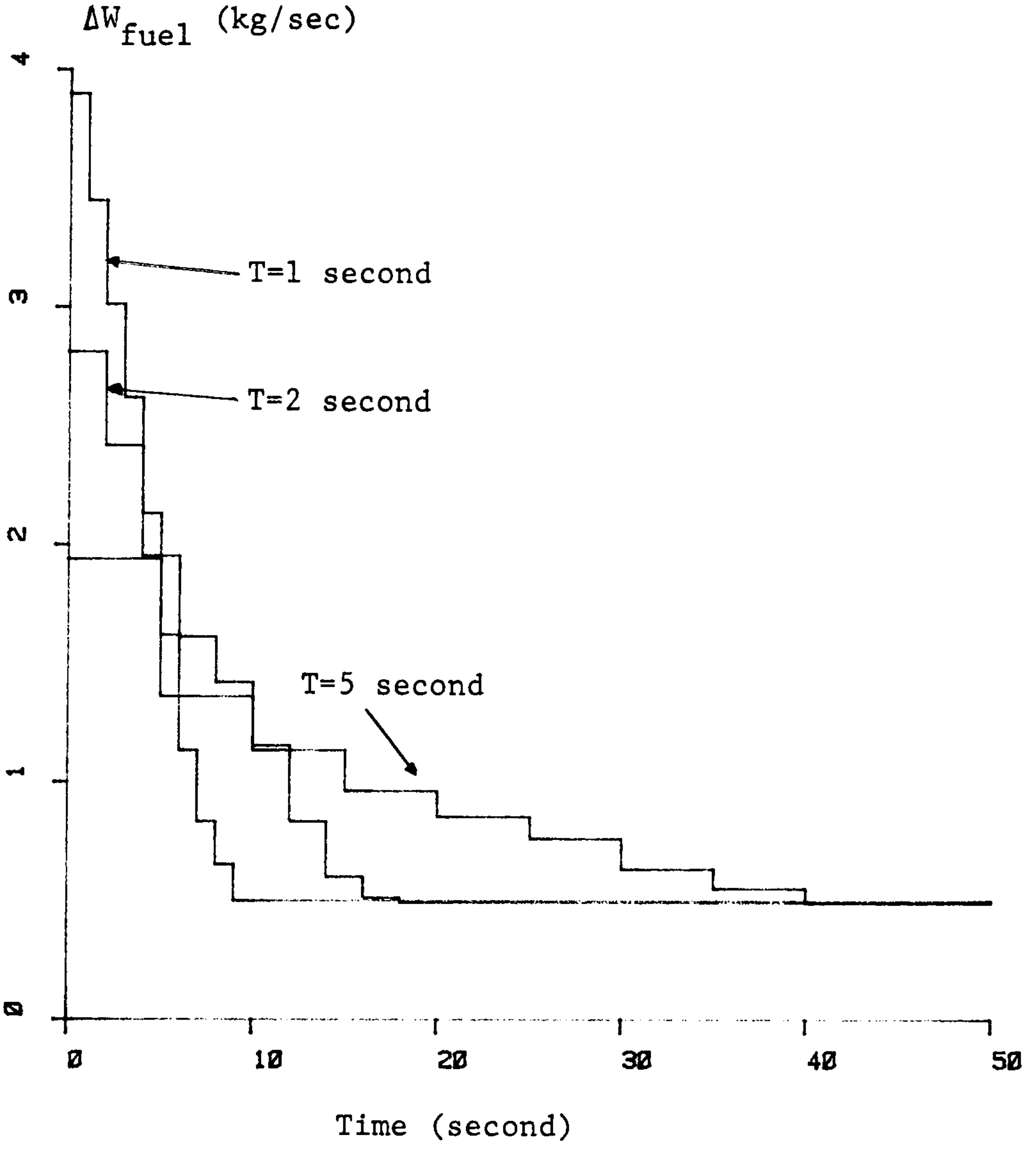

Figure 20. Fuel input rate change for digital control

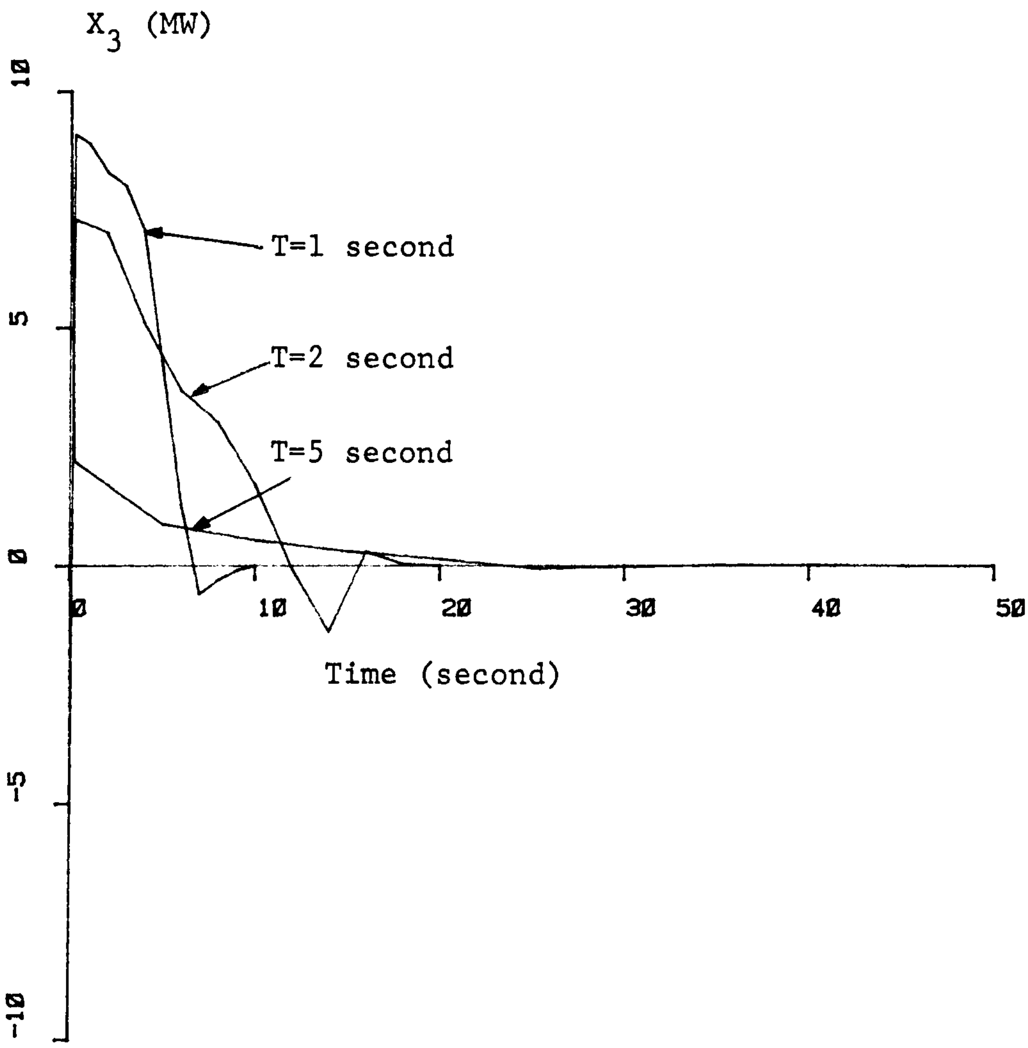

Figure 21. Power mismatch for digital control

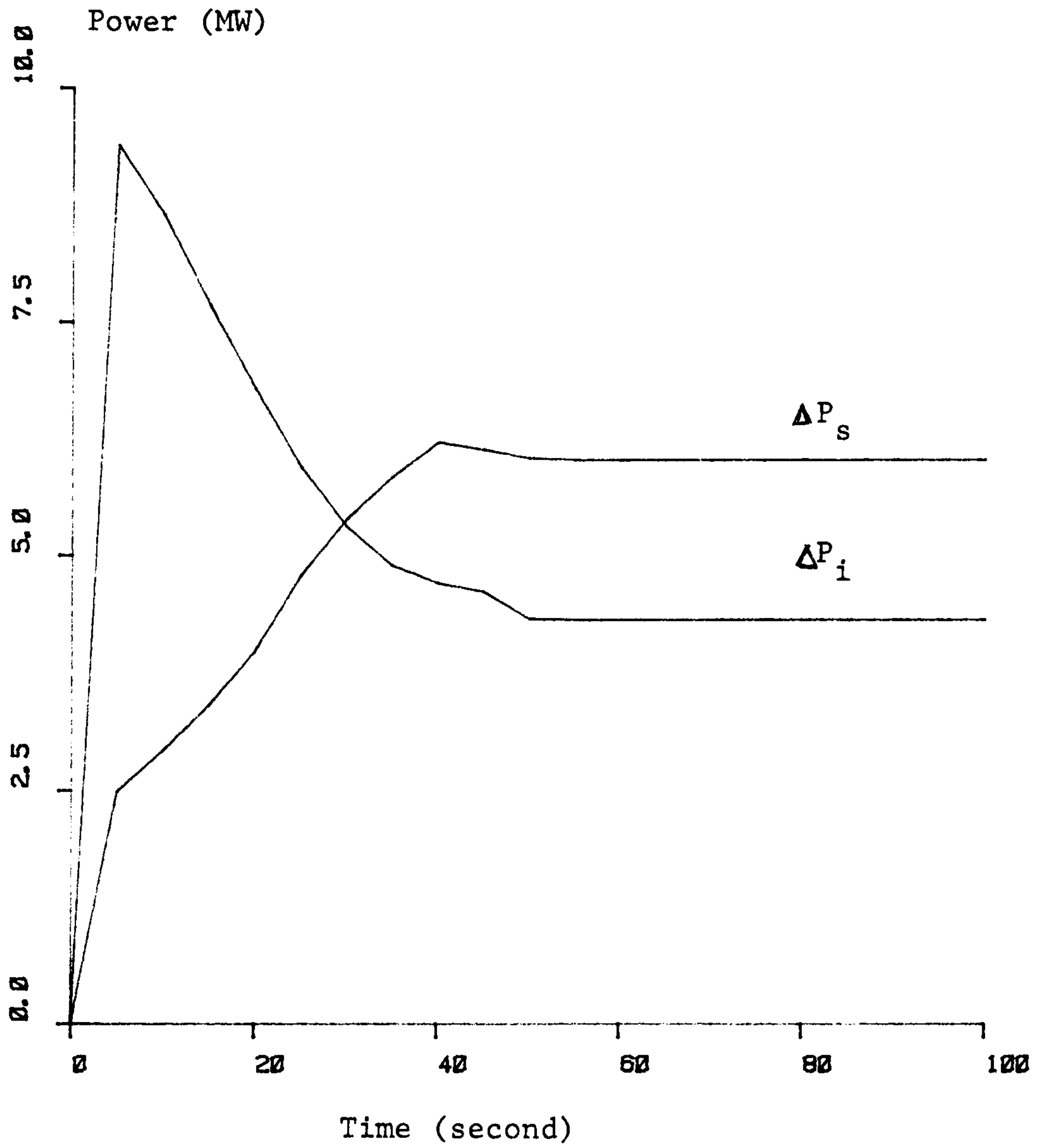

Figure 22. Load division for digital control
T = 5 second

TABLE 8

DIGITAL CONTROL PERFORMANCE

Sampling period T seconds	Frequency Error e_f $sec.^{-1}$	Total Control Effort, e_u $kg.^2 sec^{-1}$	Peak Control Effort, p_u $kg.sec^{-1}$
0.1	0.8933	54.44	12.65
1.0	0.2612	52.16	3.90
2.0	0.1917	49.06	2.81
5.0	0.0317	49.04	1.94

an increase in T. This is because the deviations in f and W_{fuel} take place at a very fast rate for low values of T and their peak values are also very high. However for low values of T, the system settles to the new steady state in a lower amount of time.

Based on the peak control effort values, it is noted that T below 2 seonds is unacceptable. This is due to the maximum limit of 2.72 kg/sec imposed on ΔW_{fuel}. Compared to PID and optimal controllers the frequency error here is more but limited to a predetermined time. The control effort does not differ significantly from the best PID and optimal controllers. However, the digital control presents a reliable, inexpensive and flexible on-line control technique for the combined plant.

A value of T = 5 seconds is an acceptable sampling time. It provides a reasonable frequency response with low control effort. It is to be noted here that the period of 5 seconds is long enough for all the computation. The digital control is expected to be implemented using a large number of dedicated microprocessors connected to a large digital computer. The digital control technique is recommended as one of the suitable control strategies for the combined plant.

CHAPTER VII

CONCLUSIONS

It was the purpose of this work to develop an incremental power model for a commercial scale, coal fired open-cycle MHD/Steam power plant and use it to study associated control problems. The model was constructed assuming the load demand changed only the state variables in a small region around the normal operating point. Various control schemes, including classical and modern schemes, were then used to force the system to a new steady state when a step change in load is received.

Classical control technique utilized the proportional-integral-derivative control to improve the response to a step change in power demand. This utilized a single state variable feedback to control the fuel input to the MHD combustor. Optimal state variable feedback was used to minimize a cost function related to the total frequency error and total control effort in a certain proportion. This involved the use of a multivariable feedback for control. Finite-time settling control algorithm for a finite settling time was also applied to a discrete form of the incremental power model. This drives the system to the new steady state in a finite time based on the sampling period chosen.

Based on the frequency error, total control effort and peak control effort criteria the following plant control schemes were chosen as being most suitable:

PID	$20/s + 10 + 10s$
Optimal	$\alpha = 1000$
Digital	$T = 5.0$ seconds

All these controllers provide acceptable values of e_f, e_u and p_u.

Digital control techniques have the advantage in real time control with a fairly inexpensive computer as the control element. For a commercial scale plant, digital control is recommended since it is more easily implemented, and is easy to maintain. However, PID and optimal control with a proper choice of parameters are acceptable if the algorithms required can be implemented closely by a digital computer.

BIBLIOGRAPHY

BIBLIOGRAPHY

1. Wu, Y. C. L., "Performance Theory of Diagonal Conducting Wall Generators," AIAA Journal, Vol. 14, No. 10, pp. 1362-1368, October 1976.

2. Louis, J. F., Kovbasyuk, V. I., "MHD Generators," in Open-cycle Magnetohydrodynamic Electrical Power Generation, Argonne : Argonne National Laboratory, 1978, pp. 157-163.

3. Hoover, D. Q., et al., "Energy Conversion Alternatives Study," Westinghouse Phase I Final Report, Vol. VIII, NASA Lewis Research Center, NASA CR-134941, Feburary 1976.

4. "Baseline Plant Open Cycle MHD-Steam Cycle Power Loop, System Design Description," Gilbert Associates, Inc. and STD, Inc. Prepared for ERDA, MHD Division, June 1976.

5. Corman, J. C., et al., "Energy Conversion Alternatives Study," General Electric Phase I Final Report, Vol. II, NASA Lewis Research Center, NASA CR-134948, Feburary 1976.

6. Wu, Y. C. L., "On Diagonal Conducting Wall MHD Generators," J. B. Dicks and Associates, Inc., Tullahoma, Tennessee, November 1976.

7. Balzhiser, R. E., "R & D Status Report : Fossil Fuel and Advanced Systems Division," EPRI Journal, Vol. 4, No. 10, pp. 36-38, October 1979.

8. Dicks, J. B., "Review of Central Power MHD," AIAA Paper, No. 75-264, 1975.

9. Chapman, J. N., "On the Economic Optimization of the MHD-Steam Power Plant," Ph.D. dissertation, The University of Tennessee, Knoxville, 1977.

10. Hals, Finn A., "Parametric Study of Potential Early Commercial MHD Power Plant," Avco Everett Research Laboratory, Inc., NASA Lewis Research Center, NASA CR-159633, December 1979.

11. Hollis, J. R., et al., "Parametric Study of Potential Early Commercial MHD Power Plant," The University of Tennessee Space Institute, NASA Lewis Research Center, 1980 (To be published).

12. Oliver, D. A., Byer, D. H., "Physical and Economic models of Open Cycle Coal Burning MHD Power Generation System," Gas Turbine Laboratory, MIT, June 1972.

13. Zygielbaum, P. S., "Operational Analysis of Open Cycle MHD," Westinghouse Research and Development Center, Research Project 639-1, June 1977.

14. Robles, T. C., "A Simulation Approach to a MHD Steam Electrical Power Generation System," Ph.D. dissertation, Montana State University, 1975.

15. Aspens, J. D., "Magnetohydrodynamic/Steam System Dynamic Modeling and Control," Ph.D. dissertation, Montana State University, 1976.

16. Agarwal, Anant, "On Modeling and Control of MHD-Steam System," M.S. Thesis, The University of Tennessee, Knoxville, 1980.

17. Elgerd, O. I., "Electric Energy Systems Theory," New York : McGraw-Hill, 1971.

18. Wu, Y. C. L., "DESIGN3 : Numerical Solution Program," The University of Tennessee Space Institute, Tullahoma, Tennessee, 1980.

19. Tyle, Navin, "Magnetohydrodynamic Energy Conversion : A Design Overview," Presented at Southeastern Regional Student Conference, AIAA, April 1980.

20. Gordon, S., McBride, B. J., "Computer Program for Calculation of Complex Chemical Equilibrium Compositions, Rocket Performance, Incident and Reflected Shocks, and Chapman-Jouguet Detonations," NASA SP-273, 1971.

21. Petrick, M., Shumyatsky, B. Ya., "Open-cycle MHD Electrical Power Generation," Argonne : Argonne National Laboratory, 1978, pp. 275-320.

22. "Engineering Test Facility Conceptual Design," Final Report, Part 2, Avco Everett Research Laboratory, Inc., June 1978, pp. 704-711.

23. Arrillaga, J., Duke, R. M., "A Static Alternative to the Transformer On-Load Tap Changer," IEEE Transactions on Power Apparatus and Systems, Vol. PAS-99, No. 1, pp. 86-91, January-February 1980.

24. Chen, T., Galle, K. R., "Transfer Functions for Steam Generating Heat Exchangers," ISA Transactions, Vol. 3, No. 4, pp. 175-183, April 1964.

25. Speckhart, F. H., Green, W. L., "A Guide to using CSMP," Englewood Cliffs, New Jersey : Prentice-Hall, Inc., 1976.

26. Ogata, K., "Modern Control Engineering," Englewood Cliffs, New Jersey : Prentice-Hall, Inc., 1970.

27. Gupta, S. C., "Transform and State Variable Methods in Linear Systems," Huntington, New York : R. E. Krieger Publishing Co., 1971, pp. 186-324.

28. Athans, M., Falb, A., "Optimal Control," New York : McGraw-Hill, 1966, pp. 771.

29. Kirk, D. E., "Optimal Control Theory : An Introduction," Englewood Cliffs, New Jersey : Prentice-Hall, Inc., 1970, pp. 3-52.

30. Auslander, D. M., et al., "Direct Digital Process Control," Proceedings of the IEEE, Vol. 66, No. 2, pp. 199-208, Feburary 1978.

31. Joseph, Roy D., Private communication on Digital Process Control, The University of Tennessee Space Institute, Tullahoma, Tennessee, March 1980.

APPENDIX

STEADY STATE SIMULATION MODEL

This Appendix is based on the work reported in reference (11). That study considers the potential configuration of an early commercial MHD/Steam power plant. We will consider here a model developed for the study of steady state performance of a combined plant with separately fired high temperature air heaters.

Major design specifications have already been summarized in Table 2 (page 17). Figure A.1 shows the design of the plant used in steady state modeling. The stream numbers in Figure A.1 are listed in Table A.1 and are self explanatory. The major subsystems included in the model are air preheaters, MHD cycle, the heat recovery system, the seed regeneration system and the steam cycle.

The computer program was written in FORTRAN IV and was executed on IBM 370/65 computer. The program is organized in the form of subroutines that simulate various plant components. The thermodynamic properties of the plasma are found using the procedure in reference (20). The other steps are same as listed in Table 2.

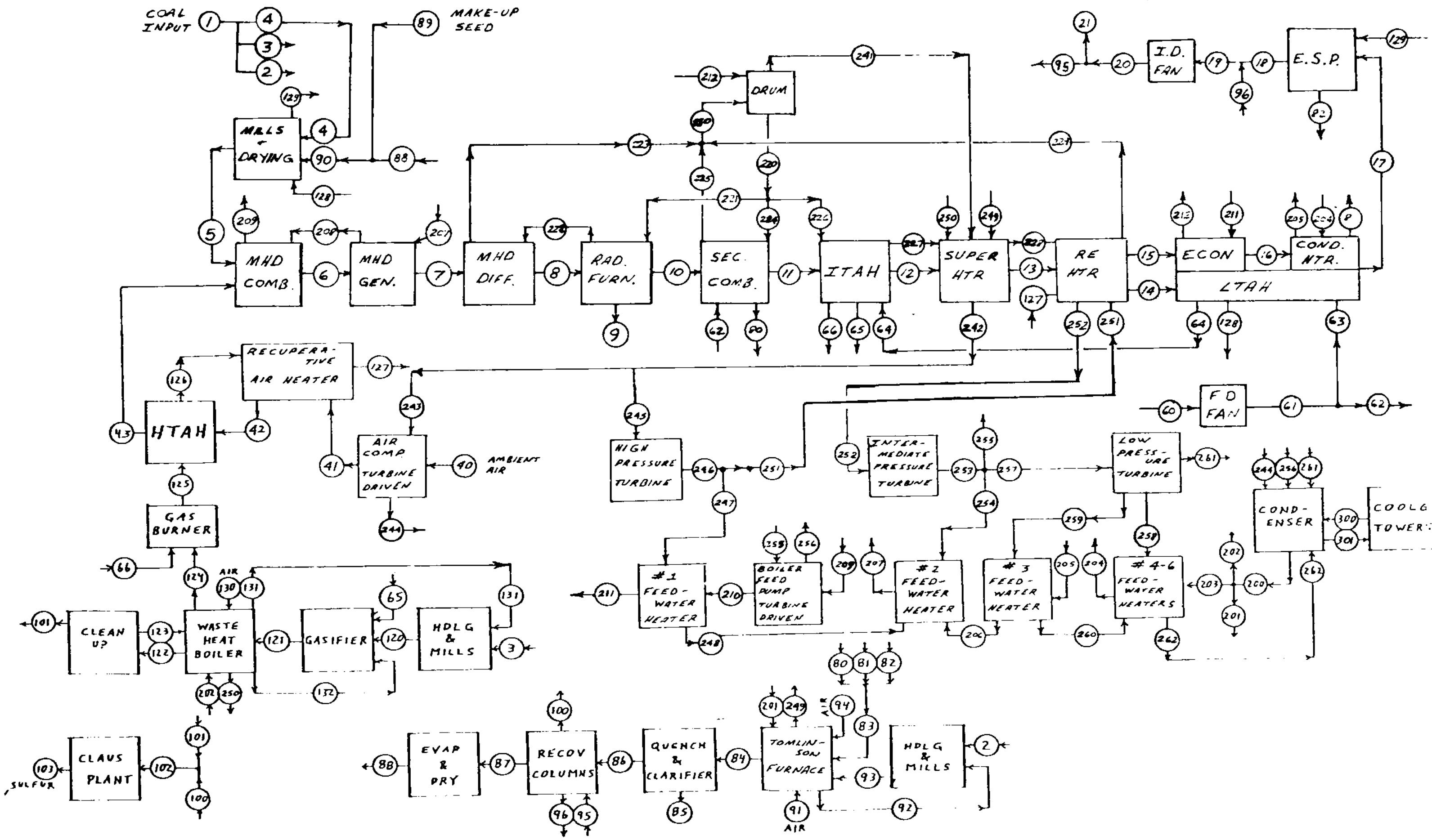

Figure A.1. Steady State Simulation Model

TABLE A.1

DESCRIPTION OF STREAM FLOWS

Stream Number	Fluid	Description
1.	Coal	Plant input
2.	Coal	To seed regeneration
3.	Coal	To gasifier
4.	Coal	To MHD Mills
5.	Input	To MHD primary combustor
6.	Flue gas	To MHD generator
7.	Flue gas	To MHD Diffuser
8.	Flue gas	To radiant furnace
9.	Slag	From radiant furnace
10.	Flue gas	From radiant furnace
11.	Flue gas	To secondary combustor
12.	Flue gas	To intermediate air heater
13.	Flue gas	To reheater
14.	Flue gas	To superheater
15.	Flue gas	To low temperature air heater
16.	Flue gas	To condensate heater
17.	Flue gas	To electrostatic precipitators
18.	Flue gas	From convection section
19.	Flue gas	To ID fan
20.	Flue gas	From ID fan
21.	Flue gas	Plant waste exit to stack
40.	Air	Inlet to air compressor
41.	HP Air	Compressor output to air heater
42.	HP Air	To HTAH
43.	HP Air	To MHD combustor
60.	Air	Inlet to FD fan
61.	Air	Discharge from FD fan
62.	Air	To secondary combustor
63.	Air	To LTAH
64.	Air	From LTAH to ITAH
65.	Air	To gasifier
66.	Air	To gas burner
80.	Ash/Seed	From secondary combustor
81.	Ash/Seed	From convection section outlet
82.	Ash/Seed	From electrostatic precipitators
83.	Ash/Seed	From seed regeneration
84.	Smelt	From Tomlinson furnace

TABLE A.1 (continued)

Stream number	Fluid	Description
85.	Dregs	Waste from clarifier
86.	Seed	To recovery columns
87.	Seed	To evaporators and spray columns
88.	Seed	Output of seed regeneration
89.	Seed	Plant supply of make-up seed
90.	Seed	To MHD seed handling
91.	Air	Inlet to seed regeneration coal handling
92.	Air	Hot air for coal handling
93.	Coal/Air	To Tomlinson furnace
94.	Air	Supply to Tomlinson furnace
95.	Flue gas	From ID fan discharge to seed
96.	Flue gas	From seed regeneration to stack
100.	H_2S	From seed regeneration
101.	H_2S	From gasifier
102.	H_2S	To Claus plant
103.	Sulfur	Output of Claus plant
120.	Coal/Air	To gasifier
121.	Gas	To waster heat boiler
122.	Gas	To clean up
123.	Gas	From clean up
124.	Gas	To gas burner
125.	Flue gas	To HTAH
126.	Flue gas	From HTAH
127.	Flue gas	To superheater
128.	Flue gas	To MHD coal drying
129.	Flue gas	Wet gas discharge
130.	Air	Supply for coal handling
131.	Air	To coal handling
132.	Char	Recycle from waste heat boiler
200.	Cond.	From condenser
201.	Cond.	To Tomlinson furnace
202.	Cond.	To waste heat boiler
203.	Cond.	To FW heater #4
204.	Cond.	To condensate heater
205.	Cond.	From condensate heater
206.	Cond.	To FW heater #2
207.	Cond.	To MHD cooling
208.	Cond.	From diffuser to channel
209.	Cond.	From channel to combustor
210.	Cond.	From MHD cooling

TABLE A.1 (continued)

Stream number	Fluid	Description
211.	BFW	From boiler feed pump
212.	BFW	To economiser
213.	BFW	To main steam drum
220.	water	Downcomer to water walls
221.	water	To water walls at radiant furnace
222.	water/Stm	To water walls at economizer
223.	water/Stm	From water walls at economizer
224.	water	To water walls at secondary combustor
225.	water/Stm	From water walls at secondary combustor
226.	water	To water walls at convection section
227.	water/Stm	Water walls from ITAH to RH
228.	water/Stm	Water walls from RH to steam drum
229.	water/Stm	From water walls at convection section
241.	Steam	From main steam drum
242.	Steam	From superheater
243.	Steam	To air compressor
244.	Steam	Air compressor turbine exhaust
245.	Steam	To HP turbine
246.	Steam	HP turbine exhaust
247.	Steam	Extraction for FW #1 heater
248.	water	Drips from FW #1 heater
249.	Steam	From Tomlinson furnace
250.	Steam	From waste heat boiler
251.	Steam	To RH
252.	Steam	To IP turbine
253.	Steam	From IP turbine
254.	Steam	To FW #2 heater
255.	Steam	To BFW turbine
256.	Steam	BFW exhaust
257.	Steam	To LP turbine
258.	Steam	To FW #4 heater
259.	Steam	From LP turbine to FW #3 heater
260.	water	To FW #4 heater
261.	Steam	LP turbine exhaust
262.	water	Drips from FW #4 heater
300.	water	To condenser
301.	water	To cooling tower

VITA

Navin Tyle was born in Bareilly, India on July 22, 1958. He attended elementary schools in Gwalior, New Delhi and Srinagar. He passed the All India Higher secondary examination in 1974 and secured first rank. For this acheivement, he received many awards, scholarships and a medal. He entered Indian Institute of Technology, Kanpur in July 1974 to pursue studies towards the degree of Bachelor of Technology with a major in Electrical Engineering. He received the B.Tech. degree with honors in April 1979. For a period of two years while an undergraduate, he worked as a Research Assistant on projects on Solar energy and Nuclear energy. After graduation, he worked as a Computer Software Engineer at Hindustan Computers Limited, New Delhi, where he worked on the development of system software for micro- and mini-computers. In September 1979, he joined The University of Tennessee Space Institute and completed the requirements for the Master of Science degree in August 1980. He plans to join Carnegie-Mellon University to work towards a Ph.D. degree in Electrical Engineering.